Single-Crystal Proton ENDOR Studies of the $[Fe_4S_4]^{3+}$ Cluster: Determination of the Spin Population Distribution and Proposal of a Model To Interpret the ^1H NMR Paramagnetic Shifts in High-Potential Ferredoxins

J.-M. Mouesca, G. Rius,† and B. Lamotte*

Contribution from the Laboratoire de Spectroscopie de Complexes Polymétalliques et de Métalloprotéines (SCPM), Service d'Etudes des Systèmes et Architectures Moléculaires (SESAM), Département de Recherche Fondamentale sur la Matière Condensée (DRFMC), Centre d' Etudes Nucléaires de Grenoble, 85X, Grenoble, 38041, France

Received July 29, 1992

Abstract: Proton ENDOR spectroscopy has been used in single crystals of the synthetic compound $[N(C_2D_5)]_2[Fe_4S_4(SCH_2C_6D_5)_4]$, which is a good biomimetic model of the active sites of many four-iron–four-sulfur proteins. The eight protons of the four thiolate CH_2 groups have been used in order to probe in detail the distribution of the unpaired electron spin population in a paramagnetic $[Fe_4S_4]^{3+}$ center created by gamma irradiation in the crystals. The thus obtained hyperfine tensors of the eight protons constitute an original, abundant, and precise source of information on this oxidation state. They have been analyzed in two separate parts. From their anisotropic parts, it is possible to deduce the distribution of the unpaired spin population on the different iron and sulfur atoms with the help of a point-dipole model. Within the limitations of the simple and symmetric vectorial spin coupling model which involves two equivalent mixed-valence iron atoms and two equivalent ferric iron atoms, we find that this paramagnetic center is close to the $|^7/_2,3,^1/_2\rangle$ state, the first number representing the spin state of the mixed-valence pair, the second one the spin state of the ferric pair, and the last one the resulting spin of the cluster. This attribution is in contrast with recent proposals considering that the $[Fe_4S_4]^{3+}$ spin state is $|^9/_2,4,^1/_2\rangle$. Finally, the analysis of the isotropic parts of the tensors leads us to propose a new quantitative model establishing the law existing between these isotropic couplings and two different parameters: a magnetic parameter which is the spin population on the adjacent iron and an angular parameter defining the orientation of each CH bond. This model seems indeed able to provide the basis of a quantitative interpretation of ^1H paramagnetic shifts in the NMR spectra of high-potential proteins in their oxidized state. Through the variety of results obtained, the interest of the present study is also that it gives the capacity to unify the interpretations of results concerning the $[Fe_4S_4]^{3+}$ state in the proteins and in model compounds which have been derived from the EPR, ENDOR, Mössbauer, and NMR spectroscopies.

(I) Introduction

Iron–sulfur proteins are ubiquitous metalloproteins present in many essential metabolic processes involving electron transfer such as photosynthesis, the respiratory chain in mitochondrial membranes, and nitrogen fixation. Their active sites correspond to diverse kinds of clusters. But those with the cubane-like Fe_4S_4 structure are the most important because they are the most common and also because they can take three different oxidation states: $[Fe_4S_4]^+$, $[Fe_4S_4]^{2+}$, and $[Fe_4S_4]^{3+}$, depending on the proteins. The magnetism of their active sites being one of their most fundamental properties, the EPR, Mössbauer, and NMR spectroscopies have been, since the beginning, privileged methods for characterizing precisely the different redox states of these proteins.[1] The interest of these methods is, in particular, that they give incisive access to the electronic structure of these clusters through different observables, such as their isomer shifts, their g and quadrupolar tensors, and more particularly through their hyperfine interactions. From this point of view, the Fe_4S_4 clusters represent particularly challenging mixed-valency systems constituted of four magnetically coupled high-spin-state iron atoms, with some kind of delocalization between them.

The present paper constitutes an important new step in the continuation of the original approach devised and developed in our laboratory with the purpose of obtaining detailed knowledge of the paramagnetic states of the Fe_4S_4 clusters. Our general purpose is to study single crystals of model compounds of the active sites of the proteins by EPR and more especially by ENDOR, in order to map the electron spin population on the different atoms of the cluster. Our method[2] consists of irradiating by gamma rays single crystals of model compounds synthesized in the $[Fe_4S_4]^{2+}$ state in order to create simultaneously, in situ, the "oxidized" species $[Fe_4S_4]^{3+}$ and the "reduced" species $[Fe_4S_4]^+$, which both remain trapped in these crystals. The first species correspond to trapped holes and the second to trapped electrons. They are oriented and diluted at relatively low concentration in the crystal matrix constituted of diamagnetic $[Fe_4S_4]^{2+}$ cubanes, thus giving the best conditions for high-resolution studies.

Two of us have inaugurated this method by a ^{57}Fe ENDOR study of a $[Fe_4S_4]^{3+}$ paramagnetic state in enriched ^{57}Fe single crystals of the $(NEt_4)_2[Fe_4S_4(SBenz)_4]$ synthetic model compound.[3] The present paper is devoted to a detailed study, this time by proton ENDOR, of the same $[Fe_4S_4]^{3+}$ paramagnetic state in the same synthetic model compound as for the previous ^{57}Fe ENDOR study. It must be said that extensive EPR studies of single crystals of this compound—and of its fully deuterated counterpart exhibiting higher resolution—show that several different $[Fe_4S_4]^{3+}$ paramagnetic species characterized by an average g-value greater than 2 are in fact created in these

† Also at the Université Joseph Fourier, Grenoble, France.

(1) (a) Lovenberg, W. *Iron-Sulfur Proteins*; Academic Press: New York, 1973; Vols. I and II; 1977; Vol. III. (b) Spiro, T. G. *Iron-Sulfur Proteins*; Wiley-Interscience: New York, 1982. (b) Matsubara, H.; Katsube, Y.; Wada, K. *Iron-Sulfur Protein Research*; Springer: Berlin, 1987. (d) Beinert, H. *FASEB J.* **1990**, *4*, 2483.

(2) Gloux, J.; Gloux, P.; Lamotte, B.; Rius, G. *Phys. Rev. Lett.* **1985**, *54*, 599.

(3) Rius, G.; Lamotte, B. *J. Am. Chem. Soc.* **1989**, *111*, 2464.

0002-7863/93/1515-4714$04.00/0

irradiated crystals, while two different $[Fe_4S_4]^+$ species having an average g-value lower than 2 are also observed.[4] The center studied here, that we have labeled center IV, is the most intense in the EPR spectra.[4] It is, hence, the first of these species that we study in such detail. The ENDOR study of another $[Fe_4S_4]^{3+}$ center created in the same crystals, called center I, is now nearly completed.[5] The fact that similar studies on the other $[Fe_4S_4]^{3+}$ and $[Fe_4S_4]^+$ species are also potentially possible demonstrates the richness of possibilities that these irradiated crystals offer. In fact, the practical limitations which might impede complete studies of all these species may come from the existence of severe overlaps in their EPR and ENDOR spectra and also from problems of sensitivity in ENDOR for those which have not very intense EPR lines.

The $[Fe_4S_4]^{3+}$ state on which the present study is focused corresponds to the oxidized state of iron–sulfur one-electron carriers working on the $[Fe_4S_4]^{2+}/[Fe_4S_4]^{3+}$ redox couple called the high-potential (or HiPIP) proteins. After the first X-ray studies of their structure,[6] these proteins have been studied by EPR[7] and ENDOR.[8] But the essential information concerning hyperfine interactions in their active sites has come from ^{57}Fe Mössbauer measurements.[9-11]

Due to the higher resolution offered by ENDOR in single crystals with respect to Mössbauer, our recent study of center IV by ^{57}Fe ENDOR[3] has provided more precise and complete information than before. However, the anisotropic parts of these tensors appeared difficult to interpret, especially the directions of their principal axes. This initial choice of the ^{57}Fe nuclei as probes was a natural one, since these nuclei belong to the atoms located at the *heart* of the system and at the origin of the magnetism in the cubane structure. But alternative and complementary choices based on other nuclei having non-zero nuclear spins are indeed possible. *The possibility that we have chosen here is to use the eight protons of the four CH_2 groups of the benzyl thiolate ligands as probes.* This is an attractive possibility, since these protons can be seen as a series of *peripheral probes* giving eight different points of view on the spin distribution, each proton being principally sensitive to the spin population on its closest iron atom. This is also an efficient choice because *a total of forty independent components are available to measure this spin distribution* through the five components of the anisotropic parts of their tensors. We will also see that the anisotropic parts of the proton tensors are simpler to interpret than those of the ^{57}Fe tensors. In effect, these protons are more distant from the electron spin population considered than the ^{57}Fe nuclei are and, moreover, their tensors are thus much less affected by orbital contributions to the hyperfine interactions.

Another incentive to the choice of these protons as probes is that the measurements of their isotropic hyperfine couplings in this model compound gives to us *the possibility to elaborate a model for the quantitative interpretation of the positions of the NMR lines of the β-CH_2 protons of cysteines in the high-potential ferredoxin proteins.* In effect, the interpretation of the NMR spectra of iron–sulfur proteins is less advanced than that for hemoproteins and their qualitative understanding has significantly progressed only very recently. Up to now, the most often discussed problem in the ferredoxins and high-potential proteins has been the temperature dependences of the paramagnetically shifted proton NMR lines. Their first interpretation was given by Dunham et al.[12] in the simplest case corresponding to the two iron and two sulfur ferredoxins. Recently, Bertini, Luchinat, et al.[13] have developed further this interpretation concerning these ferredoxins and they have extended it to the qualitative interpretation of the temperature dependence of the corresponding shifts in the oxidized state of the four iron–four sulfur high-potential ferredoxins. They have also been able to assign the corresponding NMR lines pairwise to β-CH_2 groups of cysteins,[14,15] to propose an interpretation of the sign of their shifts by reference to the spin coupling model,[14,15] and also to assign these protons in the high-potential protein of *Chromatium vinosum*.[16] Besides, very recently, nearly complete sequential resonance assignments of this protein have been performed by Nettesheim et al. in its oxidized state[17] and by Gaillard et al. in its reduced state.[18]

But it remains that, at the present time, no really quantitative model exists to interpret the paramagnetic shifts of these protons in the iron–sulfur proteins. We hope that the present study will contribute to its elaboration by taking advantage of the fact that, in this synthetic model, the CH_2 proton positions are well defined and that their hyperfine tensors can be precisely determined and attributed, their isotropic parts being constitutive elements of the paramagnetic NMR shifts.

In summary, after the presentation of the experimental determination of the hyperfine tensors of the eight protons of the CH_2 groups, this article will analyze successively the two parts into which these tensors can be decomposed: The anisotropic part of these tensors due to the electron–nuclear spin dipolar interactions will give, via the point-dipole model, the distribution of the unpaired electron spin population, and this distribution will be discussed in terms of the spin vector model already used in the literature. The isotropic parts of these tensors will be discussed in relation to the known geometry of the ligands, and they will permit us to deduce an empirical law relating their values to the directions of the C–H bonds. The adequacy of this law for the interpretation of the paramagnetic NMR shifts of the β-CH_2 protons in the oxidized state of the high-potential proteins will then be discussed.

(II) Experimental Section

The resolution that we can attain with these ENDOR experiments is much higher than in EPR or Mössbauer; but it is however limited when, as is the case here, we have to consider small hyperfine interactions for a rather great number of nuclei. An important condition of success is thus that the ENDOR spectra just contain the transitions corresponding to the protons of interest. This is why we have been obliged to substitute by deuterium any other proton than those pertaining to the CH_2 groups in the compound used for this study, since these eight protons already give 32 ENDOR lines for a general orientation. Consequently, *we have synthesized benzyl thiolate ligands selectively deuterated on their phenyl ring and also fully deuterated tetraethylammonium counterions for the purpose of this study.*

(4) Gloux, J.; Gloux, P.; Lamotte, B.; Mouesca, J.-M.; Rius, G. To be published.
(5) Mouesca, J.-M.; Lamotte, B.; Rius, G. To be published.
(6) Carter, C. W., Jr. In *Iron-Sulfur Proteins*; Lovenberg, W., Ed.; Academic Press: New York, 1977; Vol. III, p 158.
(7) (a) Antanaitis, B. C.; Moss, T. H. *Biochim. Biophys. Acta* **1975**, *405*, 262. (b) Peisach, J.; Orme-Johnson, N. R.; Mims, W. B.; Orme-Johnson, W. H. *J. Biol. Chem.* **1977**, *252*, 5643. (c) Dunham, W. R.; Hagen, W. R.; Fee, J. A.; Sands, R. H.; Dunbar, J. B.; Humblet, C. *Biochim. Biophys. Acta* **1991**, *1079*, 253.
(8) Anderson, R. E.; Anger, G.; Petersson, L.; Ehrenberg, A.; Cammack, R.; Hall, D. O.; Mullinger, R.; Rao, K. K. *Biochim. Biophys. Acta* **1975**, *376*, 63.
(9) Dickson, D. P. E.; Johnson, C. E.; Cammack, R.; Evans, M. C. W.; Hall, D. O.; Rao, K. K. *Biochem. J.* **1974**, *139*, 105.
(10) Middleton, P.; Dickson, D. P. E.; Johnson, C. E.; Rush, J. D. *Eur. J. Biochem.* **1980**, *104*, 289.
(11) Papaefthymiou, V.; Millar, M. M.; Münck, E. *Inorg. Chem.* **1986**, *25*, 3010.
(12) Dunham, W. R.; Palmer, G.; Sands, R. H.; Bearden, A. J. *Biochim. Biophys. Acta* **1971**, *253*, 373.
(13) (a) Banci, L.; Bertini, I.; Luchinat, C. *Struct. Bonding (Berlin)* **1990**, *72*, 113. (b) Banci, L.; Bertini, I.; Briganti, F.; Luchinat, C. *New J. Chem.* **1991**, *15*, 467.
(14) Bertini, I.; Briganti, F.; Luchinat, C.; Scozzafava, A.; Sola, M. *J. Am. Chem. Soc.* **1991**, *113*, 1237.
(15) Banci, L.; Bertini, I.; Briganti, F.; Luchinat, C.; Scozzafava, A.; Vicens Oliver, M. *Inorg. Chem.* **1991**, *30*, 4517.
(16) Bertini, I.; Capozzi, F.; Ciurli, S.; Luchinat, C.; Messori, L.; Piccioli, M. *J. Am. Chem. Soc.* **1992**, *114*, 3332.
(17) Nettesheim, D. G.; Harder, S. R.; Feinberg, B. A.; Otvos, J. D. *Biochemistry* **1992**, *31*, 1234.
(18) Gaillard, J.; Albrand, J.-P.; Moulis, J.-M.; Wemmer, D. E. *Biochemistry* **1992**, *31*, 5632.

(1) Preparation of $C_6D_5CH_2SH$. The synthesis from perdeuterated bromobenzene of this selectively deuterated benzyl thiolate required five successive reactions: Deuterated benzoic acid was first prepared[19] by the Grignard reaction of magnesium with perdeuterated bromobenzene to give the C_6D_5MgBr adduct. By reaction with CO_2, we obtained $C_6D_5CO_2MgBr$, the decomposition of this Grignard reactant giving the deuterated benzoic acid. In the second step, methyl benzoate selectively deuterated on the benzene ring was obtained by reaction of purified thionyl chloride with a mixture of absolute (nondeuterated) methyl alcohol and the previously prepared deuterated benzoic acid.[20] The so-obtained methyl benzoate was taken out by distillation. It was then reduced under anhydrous conditions by $LiAlH_4$ to give benzyl alcohol only deuterated on the phenyl ring,[21] which was extracted by a second distillation. Then, the corresponding benzyl chloride[21] was obtained by reaction of thionyl chloride on this deuterated benzyl alcohol. Finally, by successive additions of this benzyl chloride to magnesium in dry diethyl ether and of sulfur dissolved in dry benzene to this mixture, we prepared the $C_6D_5CH_2SMgCl$ Grignard compound.[22,23] Its decomposition with acidified water gave us the selectively deuterated benzyl thiol,[23] which was extracted by distillation. However, the corresponding disulfide was also obtained. This disulfide was reduced separately by $LiAlH_4$,[24] in order to complete the quantity of $C_6D_5CH_2SH$ obtained. We verified by NMR that deuteration of the phenyl ring was of 98%. This preparation started with 50 g of perdeuterated bromobenzene, and we have obtained 6.3 g of the $C_6D_5CH_2SH$ benzyl thiol, the global yield being thus 16%.

(2) Preparation of $(C_2D_5)_4NI$. (a) Preparation of $(C_2D_5)_3N$. Perdeuterated triethylamine was prepared by reaction of deuterated acetonitrile with D_2 under pressure, palladium on coal being used as catalyst.[25] We observed that this reaction gives generally a mixture of the deuterated monoethylamine, diethylamine, and triethylamine with also deuterated ammonia. Preliminary trials made under various conditions of temperature and pressure permitted us to find that a pressure of 200 bar and a temperature of 150 °C maximized the formation of the deuterated triethylamine. Under these conditions, the monoethylamine was not formed. Deuterated ammonia was eliminated from the mixture by reaction with diluted hydrochloric acid, evaporation, dissolution in ethyl alcohol, and separation of the insoluble ammonium chloride. The deuterated triethylamine was regenerated by reaction with aqueous sodium hydroxide. NMR analysis indicated that the compound so-prepared contained 10% of deuterated diethylamine; this impurity was eliminated by heating the mixture to reflux with benzoic anhydride. The pure perdeuterated triethylamine was finally recovered by distillation.

(b) Preparation of C_2D_5I. Perdeuterated ethyl iodide was prepared by reaction of perdeuterated ethyl alcohol with phosphorus and iodine[26] and purified by distillation under argon.

(c) Preparation of $(C_2D_5)_4NI$. The perdeuterated tetraethylammonium iodide was obtained by reaction of the (as prepared above) perdeuterated triethylamine and ethyl iodide compounds.[25] We verified by NMR that this final compound is deuterated at 98%.

(3) Preparation of $[(C_2D_5)_4N]_2$ $[Fe_4S_4(SCH_2C_6D_5)_4]$. Using the perdeuterated tetraethylammonium iodide prepared above, the iron–sulfur complex $[(C_2D_5)_4N]_2$ $[Fe_4S_4(S\text{-}t\text{-}Bu)_4]$ was prepared, following the synthesis procedure of Christou and Garner.[27] The final compound was obtained by ligand exchange with $C_6D_5CH_2SH$ in acetonitrile.[27] The different steps of the preparation of this complex were conducted in a glovebox under an argon atmosphere (1 ppm of O_2).

(4) Preparation of Crystal Samples. Single crystals weighing between 6 and 8 mg were obtained by a transport method in a solution of the compound in acetonitrile.[3] These crystals were then irradiated to doses between 400 and 700 Mrad by γ rays in a ^{60}Co source at room temperature, under an argon atmosphere.

The crystallographic structure of this compound has been published by Averill et al.[28] It crystallizes in the monoclinic space group $P21/c$ with $Z = 4$. The single crystals generally grow with a well-developed face corresponding to the *ac* plane, with its greatest dimension along the *a* axis. An orthogonal reference frame axis *a*, *b*, and *c** is defined from this morphology, the last axis being defined as perpendicular to the two others. These elements are used to orient our single crystals and to study their EPR and ENDOR spectra in the three perpendicular planes *ab*, *bc**, and *ac**. In these crystals, each paramagnetic center has two inequivalent sites for a general orientation of the static magnetic field with respect to the orientations of the unit cell. These two sites become equivalent in the EPR and ENDOR spectra when the magnetic field vector is either contained in the mirror glide plane *ac* or is aligned along the *b* screw axis.

(5) EPR and ENDOR Methodology. The ENDOR experiments were performed on a BRUKER ER 200 D-SRC spectrometer equipped with the VARIAN E 1700 broad-band ENDOR accessory and a 100-W ENI 3100 L broad-band power amplifier. It was driven by a Hewlett Packard computer HP 9153, through a home-made interface. The single crystals were maintained for these experiments at temperatures around 10 K in the spectrometer with the help of an Oxford instruments ESR-9 continuous-flow helium cryostat. The ENDOR spectra were detected with amplitude modulation of the radiofrequency at 12.5 kHz, without field modulation. For double-ENDOR experiments, the Hewlett Packard generator–sweeper 8601 A was used.

(III) Experimental Results

As it has been said in the Introduction, the present study is dedicated to the paramagnetic center named center IV, corresponding to the oxidized state $[Fe_4S_4]^{3+}$, which two of us have already studied by ^{57}Fe ENDOR[3] and which is characterized by a **g** tensor having the following principal values: $g_1 = 2.066$, $g_2 = 2.025$, and $g_3 = 2.014$.[29]

Let us recall that the previous Mössbauer studies of the high-potential *Chromatium* protein[9,10] and of the $[Fe_4S_4(S\text{-}2,4,6\text{-}(i\text{-}Pr)_3C_6H_2)_4]^-$ model compound[11] identify in this state two distinct pairs of iron atoms called α and β. This means that the delocalization is not uniform on the four atoms of this delocalized mixed-valence cluster, since, in first approximation, it is possible to distinguish two α irons corresponding to a delocalized mixed-valence pair $Fe^{2.5+}$–$Fe^{2.5+}$ and two β irons of a ferric pair Fe^{3+}–Fe^{3+}. It is also important to recall that our previous ENDOR study of the ^{57}Fe hyperfine tensors of this center IV[3] has already permitted us to demonstrate that the mixed-valence pair is localized on the iron atoms labeled 3 and 4 in the crystallographic structure.[28]

The geometry of the cubane with its four benzyl ligands taken from the X-ray study[28] is presented in Figure 1. We have chosen to label the atoms corresponding to this structure determination, in particular for the eight protons which constitute our probes. These protons surround the cubane, and their positions are all inequivalent with respect to it. Among them, some are closer to the cubane than others. If we consider the protons 5, 6, 7, and 8 placed "on the side" of the mixed-valence pair (i.e. those belonging to the thiolate ligands bound the iron atoms 3 and 4), the protons 5 and 7 are closer to these irons than are the protons 6 and 8. Similarly, for the protons 1, 2, 3, and 4 placed on the side of the pair of ferric atoms 1 and 2, the protons 1 and 3 are closer to these irons 1 and 2 than are the protons 2 and 4.

The absolute necessity of substituting by deuterium atoms all the protons in the crystal, except those of these CH_2 groups, is illustrated in Figure 2. In this figure, we compare the ENDOR spectra of the paramagnetic center obtained along the *b* axis with

(19) Murray, A., III; Williams, D. *Organic Syntheses with Isotopes*; Interscience: New York, 1958; Part 1, p 86.
(20) Vogel, A. I. *Textbook of Practical Organic Chemistry*; Longmans Green: Harlow, U. K., 1956; p 781.
(21) Murray, A., III; Williams, D. *Organic Syntheses with Isotopes*; Interscience: New York, 1958; Part 1, p 75.
(22) Gilman. Blatt, A. H. *Organic Syntheses*; J. Wiley: New York, 1967; Vol. 1, p 471.
(23) Adams, P. T. *J. Am. Chem. Soc.* **1955**, *77*, 5357.
(24) Arnold, R. C.; Lien, A. P.; Alm, R. M. *J. Am. Chem. Soc.* **1950**, *72*, 731.
(25) Hertz, H. G.; Lindman, B.; Siepe, V. *Ber. Bunsen-Ges. Phys. Chem.* **1969**, *73*, 543.
(26) Blatt, A. H. *Organic Syntheses*; J. Wiley: New York, 1959; Collect. Vol. 2, p 399.
(27) Christou, G.; Garner, C. D. *J. Chem. Soc., Dalton Trans.* **1979**, 1093.
(28) Averill, B. A.; Herskowitz, T.; Holm, R. H.; Ibers, J. A. *J. Am. Chem. Soc.* **1973**, *95*, 3523.
(29) Following the suggestion of one reviewer, let us also recall (see ref 3) that the principal directions of the **g** tensor are such that (1) the direction corresponding to g_3 is very close (4°) to the direction joining the two irons belonging to the mixed-valence pair, i.e. the Fe_3Fe_4 direction, (2) the direction corresponding to g_2 is very close to the Fe_1Fe_2 direction, and (3) consequently, the principal direction corresponding to g_1 is parallel to the approximate $\bar{4}$ axis of the $[Fe_4S_4]^{2+}$ cubane.

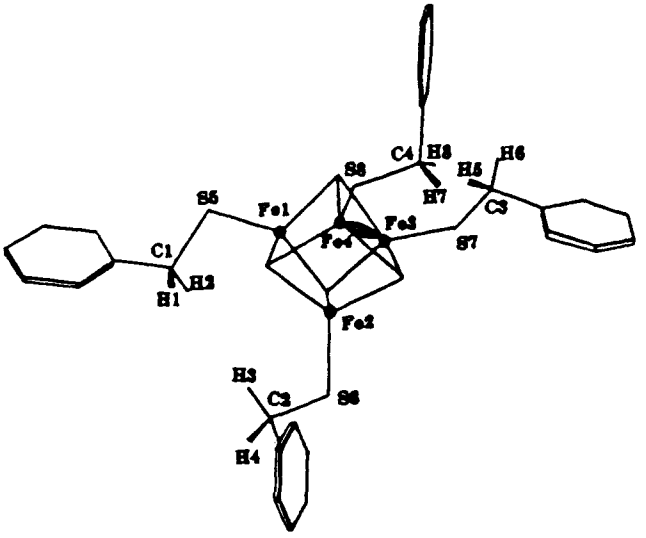

Figure 1. Structure of the Fe_4S_4 cubane with its four benzyl ligands taken from the X-ray study.[28] The mixed-valence pair is symbolized on the iron atoms 3 and 4.

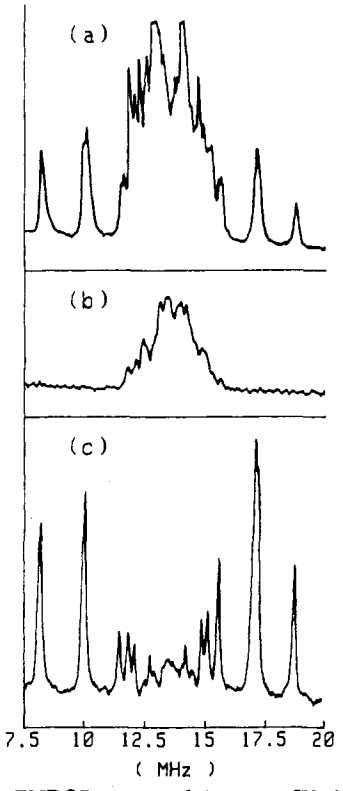

Figure 2. Proton ENDOR spectra of the center IV obtained when the magnetic field is aligned along the *b* axis of the crystal: (a) spectrum obtained with a crystal of the completely protonated compound, $[(C_2H_5)_4N]_2[Fe_4S_4(SCH_2C_6H_5)_4]$; (b) spectrum obtained with a crystal of the compound where the ligands are completely deuterated and the counterion is completely protonated, $[(C_2H_5)_4N]_2[Fe_4S_4(SCD_2C_6D_5)_4]$; (c) spectrum obtained with a crystal of the compound deuterated on the counterions and also on the phenyl rings of the ligands, $[(C_2D_5)_4N]_2[Fe_4S_4(SCH_2C_6D_5)_4]$. All the subsequent ENDOR studies have been made with this last type of crystal.

single crystals of, respectively, the fully protonated compound (Figure 2a), the compound deuterated on the benzyl ligands but with protonated tetraethylammonium counterions (Figure 2b), and the compound used for these studies having deuterated counterions and the benzyl thiolate ligands only deuterated on the phenyl rings (Figure 2c). In Figure 2a, the hyperfine structure corresponding to the four most coupled protons appears well resolved at each side of the spectrum, but its center contains a crowd of badly resolved lines. Figure 2b shows that a certain number of these ENDOR lines correspond to protons of the counterions having significant dipolar hyperfine interactions with the paramagnetic $[Fe_4S_4]^{3+}$ center studied. By contrast with the spectrum of Figure 2a, we can see that the ENDOR spectrum of the selectively deuterated compound of Figure 2c is well resolved in its central part. This demonstrates that the selective deuteration is an absolute requirement if we want to have some chance to measure the hyperfine tensors corresponding to all (or nearly all) the protons of interest.

Since even after deuteration the number of lines remains large and the resolution limited, we have been obliged to take the ENDOR spectra at every two degrees in the three orthogonal planes *ab*, *bc**, and *c*a* in order to be able to follow their angular variations. For each crystal orientation, the ENDOR spectra have been obtained by sitting at the center of the EPR line corresponding to the paramagnetic center studied. In the two planes *ab* and *bc**, the ENDOR spectra have been taken successively for the two EPR lines corresponding to the two different magnetic sites and in an angular domain of 90° between these two axes. In the mirror plane *c*a* where these two sites are equivalent, they have been traced for a range of 180°. These angular variations are reported in Figure 3a "for a fixed magnetic field", i.e. after having reset each measured ENDOR frequency to a common value ν_N^0 of the Zeeman proton frequency in order to mask in this figure the effects of the *g* anisotropy. We can see that, in spite of the great resolution inherent to the ENDOR method, we are just at the limit where it is possible to follow the angular variations of the lines associated to the different protons. Difficulties arise especially around the *a* and *c** axes and in large portions of the *ac** plane where the ENDOR lines are all packed in a small range of frequencies. The problem is particularly ticklish for the protons with the smallest hyperfine couplings corresponding to the ENDOR lines situated around the center of the spectra. This is why we have been obliged, in the most difficult portions of these angular variations, to follow the ENDOR lines at each degree.

At this stage, we want to add two pieces of information of some importance for the analysis of these results.

First, we have detected supplementary proton ENDOR lines in addition to those pertaining to the eight protons of the CH_2 groups bonded to the paramagnetic $[Fe_4S_4]^{3+}$ studied. Certain of them can be clearly seen in Figure 3a. They correspond to relatively weak hyperfine interactions which, for certain domains of orientations, are of the same order of value as some of the previous ones. We have verified that they must be attributed to the closest of the CH_2 protons of the $[Fe_4S_4(SCH_2C_6D_5)_4]^{2-}$ molecules in positions of first neighbors with respect to the paramagnetic center studied.[30]

Second, just from the raw experimental data, it has been possible to follow the angular variations of the protons having the greatest hyperfine interactions. But the situation is not so simple for the others having interactions smaller than the previous ones and pertaining either to the paramagnetic center or to the diamagnetic first neighbors just mentioned above. More often, only rather small portions of curves corresponding to certain ranges of orientations could be obtained directly for these protons with small hyperfine interactions. In effect, their ENDOR lines are masked by the other ENDOR lines and are thus invisible for the other orientations. Moreover, this situation is affected by the notorious fact that the ENDOR line intensities can vary very much and in a rather unpredictable way, as can be seen for instance in Figure 2.

(30) For more details, see: Mouesca, J.-M. *Etude par ENDOR de deux centres paramagnétiques $[Fe_4S_4]^{3+}$. Couplages hyperfins des protons et structure électronique et magnétique de ces deux cubanes.* Ph.D. Thesis, Université Joseph Fourier, Grenoble, France, 1991.

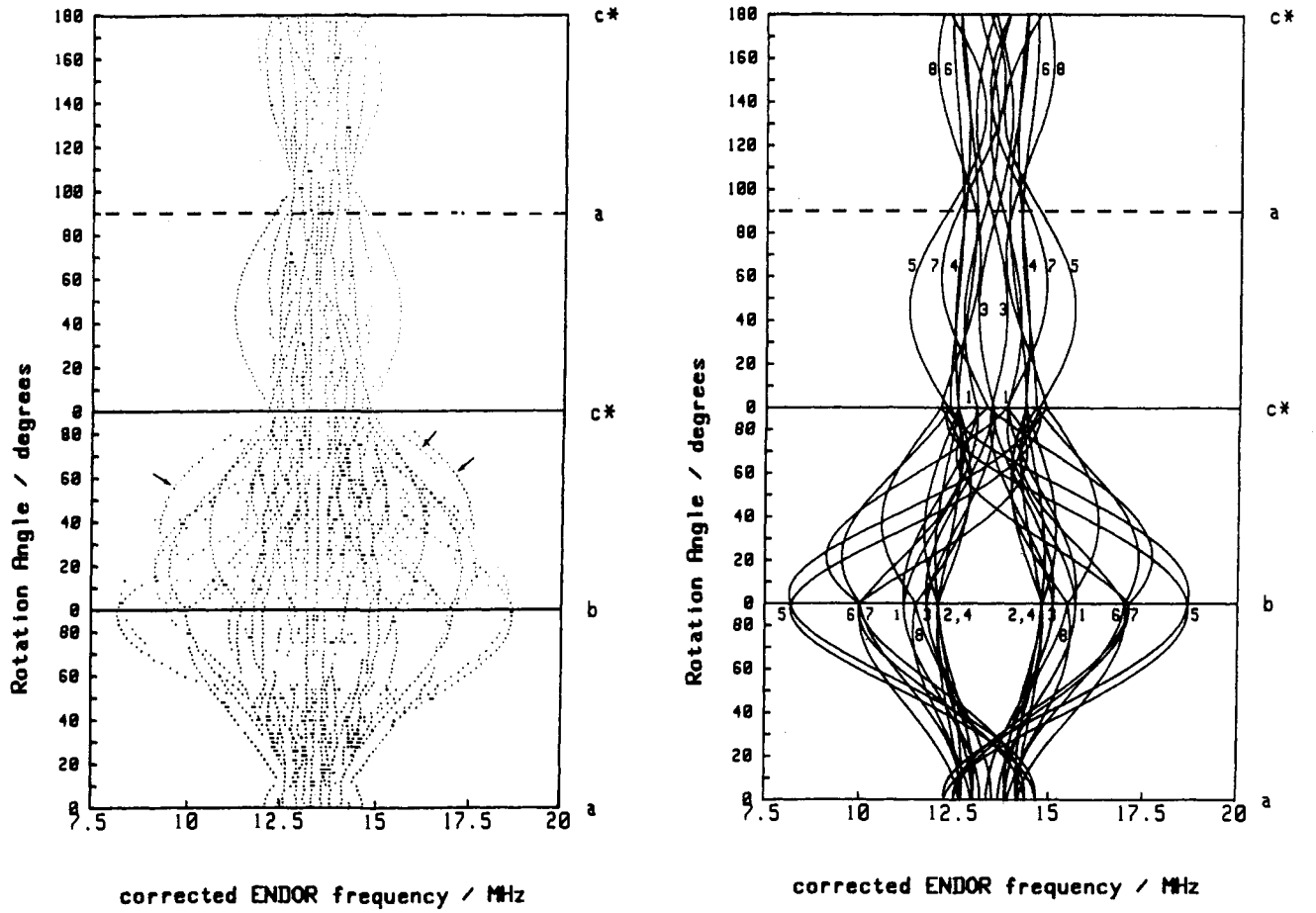

Figure 3. (a, left) Angular dependences in the three orthogonal planes *ab*, *bc**, and *c***a* of the positions of the proton ENDOR lines for the center IV. In this figure, each measured ENDOR frequency has been reset to a common value ν_N^0 of the Zeeman proton frequency. Note that the small portions of the curves marked by arrows do not belong to center IV. They are proton ENDOR lines corresponding to another paramagnetic center also present in the crystal which has its EPR line in near superposition with those of center IV in this portion of the *bc** plane. (b, right) Fits of the angular dependences of the positions of the proton ENDOR lines presented in part a.

Consequently, computer curve fitting has been practiced on the raw data of Figure 3a in order to discriminate between the different protons, to attribute each curve of angular variation of the ENDOR lines to a defined proton, and to complete the curves in the three planes by linking their separate fragments. We have used a standard fitting procedure which calculates the proton ENDOR transitions from the usual spin hamiltonian

$$H = \mu_S \vec{B}\cdot\tilde{g}\cdot\vec{S} - \gamma\vec{B}\cdot\vec{I} + \vec{I}\cdot\tilde{A}\cdot\vec{S} \qquad (1)$$

which neglects the off-diagonal hyperfine terms in the electron spin $\vec{S}$.

If the $\tilde{g}$ tensor were isotropic, the two ENDOR frequencies ν_{M_S} (where $M_S = \pm^1/_2$) would be given by

$$\nu_{M_S}^2 - \nu_N^2 = {}^1/_4\sum_{\alpha,\beta} l_\alpha l_\beta (A^2)_{\alpha\beta} - 2\nu_N M_S \sum_{\alpha,\beta} l_\alpha l_\beta A_{\alpha\beta} \qquad (2)$$

In this expression the $A_{\alpha\beta}$ are the tensorial elements of $\tilde{A}$ and the l_α are the direction cosines of $\vec{B}$ with respect to the α axis (α,β corresponding to either the *a*, *b*, or *c** directions).

Since the $\tilde{g}$ tensor is not very anisotropic, it has been proved sufficient to use the expression 2 provided that we correct the measured ENDOR frequencies (as we have said above). In effect, in any given $\alpha\beta$ plane, each so-corrected ENDOR frequency ($\nu_{M_S} - \Delta\nu_N$) was very well fitted by the following expression:

$$(\nu_{M_S} - \Delta\nu_N)^2 = a_{M_S}^{\alpha\alpha}\cos^2\theta + a_{M_S}^{\beta\beta}\sin^2\theta + 2a_{M_S}^{\alpha\beta}\cos\theta\sin\theta \qquad (3)$$

In this expression, $\Delta\nu_N = \nu_N(\theta) - \nu_N^0$ and θ is the angle between the initial axis α and the magnetic field $\vec{B}$. The $a_{M_S}^{\alpha\alpha}$, $a_{M_S}^{\beta\beta}$, and $a_{M_S}^{\alpha\beta}$ are the values that we determine by the fit.

In the $\alpha\beta$ plane, the components $A_{\alpha\alpha}$, $A_{\beta\beta}$, and $A_{\alpha\beta}$ of the $\tilde{A}$ tensor could then be obtained by the following expressions

$$A_{\alpha\alpha} = \frac{a_-^{\alpha\alpha} - a_+^{\alpha\alpha}}{2\nu_N^0}, \quad A_{\beta\beta} = \frac{a_-^{\beta\beta} - a_+^{\beta\beta}}{2\nu_N^0}, \quad A_{\alpha\beta} = \frac{a_-^{\alpha\beta} - a_+^{\alpha\beta}}{2\nu_N^0} \qquad (4)$$

where the + and − index in $a_{M_S}^{\alpha\alpha}$, $a_{M_S}^{\beta\beta}$, and $a_{M_S}^{\alpha\beta}$ stand respectively for $M_S = +^1/_2$ and $M_S = -^1/_2$ associated with the two ν_{M_S} ENDOR transitions.

In practice, a trial and error fitting procedure has been followed for each proton. The first adjustments have been made on the best experimentally determined portions of the curves of angular variations. When these calculations have been achieved for the different protons, sign ambiguities remained to be solved. They are of two kinds:

The first one is an ambiguity in the relative signs of the different components of the nondiagonalized tensors. It is due to the existence in the crystal of two inequivalent magnetic sites which become equivalent in the *ac** plane and along the *b* axis only. The problem to solve for each proton is to know how to associate the two curves of angular variation of the ENDOR lines corresponding to the two sites in the *c***b* and *ba* planes, i.e. which one in each of these planes corresponds to one site and which one corresponds to the other. In fact, this problem arises already in the EPR experiment during the determination of the **g** tensor. It was solved by determining the curves of angular variation of the EPR lines in a fourth plane (at 20° from the *b* axis), which permits one to

Table I. Principal Values and Principal Directions of the Eight Hyperfine Tensors of the Protons of the CH_2 Groups Measured by ENDOR for the $[Fe_4S_4]^{3+}$ Center IV[a]

	principal values (in MHz)			principal directions: direction cosines with respect to		
tensors	total	isotropic part	anisotropic part	$\vec{a}$	$\vec{b}$	$\vec{c}^*$
	−4.59		−2.64	−0.022	+0.994	−0.104
A_1	+0.24	−1.95	+2.19	+0.765	−0.051	−0.642
	−1.50		+0.45	+0.644	+0.094	+0.759
	(−3.5)		(−1.7)	(+0.06)	(+0.84)	(−0.54)
A_2	(−0.8)	(−1.8)	(+1.0)	(+0.93)	(−0.25)	(−0.27)
	(−1.1)		(+0.7)	(+0.36)	(+0.49)	(+0.74)
	−3.38		−2.34	−0.028	+0.993	−0.116
A_3	+0.99	−1.04	+2.03	+0.714	−0.061	−0.697
	−0.73		+0.31	+0.699	+0.102	+0.707
	−2.95		−0.92	−0.057	+0.936	+0.347
A_4	−1.21	−2.00	+0.83	+0.765	+0.264	−0.587
	−1.95		+0.09	+0.641	−0.232	+0.731
	+10.57		+8.71	+0.048	+0.996	−0.082
A_5	−4.41	+1.86	−6.27	+0.702	+0.025	+0.711
	−0.58		−2.44	+0.710	−0.091	−0.698
	+7.89		+4.26	−0.077	+0.932	+0.355
A_6	+1.37	+3.63	−2.26	+0.657	+0.315	−0.685
	+1.63		−2.00	+0.750	−0.180	+0.636
	+8.60		+7.00	+0.026	+0.930	−0.366
A_7	−3.34	+1.60	−4.95	+0.707	+0.242	+0.665
	−0.45		−2.05	+0.707	−0.276	−0.651
	+5.95		+3.35	+0.201	+0.773	−0.602
A_8	+0.65	+2.60	−1.95	+0.887	+0.117	+0.447
	+1.20		−1.40	+0.416	−0.623	−0.662

[a] The values given for the tensor A_2 have been put between parentheses, since they are much less sure than the others (see the text).

connect in the correct way the curves corresponding to the same site in the two planes c^*b and ba. Then the problem is automatically solved for the ENDOR set of angular variations because, during the ENDOR experiment, one sits on a particular EPR line associated with a defined site generally well separated from the other.

The second kind of ambiguity concerns the signs of the hyperfine interactions themselves. Anticipating that the point-dipole model is a good approximation in the present case (see in Section IV-2), the signs under discussion are those of the component of the traceless tensor of each proton which has the largest magnitude. Their absolute values cannot be deduced from the ENDOR experiments alone, but double-ENDOR experiments[31] give the possibility to obtain the relative signs of the hyperfine couplings corresponding to the different protons. We have already used this method in our previous article where this paramagnetic center was studied by ^{57}Fe ENDOR.[3] The same method has been used here for the orientations of the crystal where the ENDOR lines of the different protons are sufficiently separated: along the b axis and in the bc^* and ba planes, not far from the b axis. But the problem of the determination of the absolute signs of the hyperfine tensors remains. In practice, we have solved it through the procedure developed in Section IV-3, permitting one, with the help of the point-dipole model, to deduce the distribution of the spin populations from the analysis of the anisotropic parts of the tensors. The signs so-obtained correspond to those of the tensors given in Table I; their comparisons between the different protons agree with their relative signs that we had determined by the double-ENDOR experiments.

These calculations mentioned above have also constituted the basis of our assignments of the different tensors to the eight protons of interest. This was done by successive series of trial and error tests for the four protons 1, 3, 5, and 7 respectively close to the Fe_1, Fe_2, Fe_3, and Fe_4 atoms, in a first step. We have compared the principal directions and principal values thus obtained with the experimental ones. Relying on this first assignment, the expected tensors for the protons 2, 4, 6, and 8 (which are somewhat more distant from these irons) were then calculated with the point-dipole model. This permitted in a straightforward way their identification to the measured ones (except for the proton 2, see the discussion below). It was thus possible to obtain by this way an ensemble of proton hyperfine tensors giving the best fits for all the experimental ENDOR angular variation curves discussed above and to obtain also the attribution of these tensors to the different protons labeled in this structure. This set of proton hyperfine tensors is presented, after diagonalization, in Table I.

We must remark that all the tensors reported in Table I are not determined with the same quality, since we work just at the limit of resolution (and even below, in some cases...). We consider that those associated with the protons 4, 5, 6, 7, and 8 have been determined without any ambiguity, but that we have met some variable difficulties with the three others. Only minor uncertainties remain for the tensors of the protons 1 and 3, but they only imply less precision in their determination, their ENDOR transitions being masked by those of other protons for large parts of the orientations. The problem is more serious for the proton 2, which has been essentially derived by computer fitting and by the use of the models developed in the Sections IV-2 and IV-3. Hence, its tensor must be considered with less certainty than those corresponding to the other protons, and it is certainly much more approximate.

Before developing quantitative analyses of these tensors, we find it useful to make several remarks about the results contained in Table I. The first one is that the principal direction corresponding to the greatest principal value is very close to the b axis direction of the crystal for six out of eight of the tensors, as the characteristic anisotropy of the ENDOR curves indicates in Figure 3a. This observation agrees with the positions of the cubanes and of their ligands in the crystal, since the directions joining each proton to its closest iron are more or less along the direction of the b axis. It also indicates that the major part of the unpaired spin population is located on the iron atoms.

The second feature apparent in Table I is that the protons 5, 6, 7, and 8 belonging to the ligands placed on the side of the Fe_3 and Fe_4 atoms of the cluster (see Figure 1) are also those having the greatest anisotropic tensors. This confirms that, for this center IV, these irons 3 and 4 constitute the mixed-valence pair bearing the greatest part of the unpaired spin population, as we have already concluded in our previous ^{57}Fe ENDOR study.[3] Moreover, the protons 5 and 7 have greater anisotropic tensors than

(31) Cook, R. J.; Whiffen, D. H. *Proc. Phys. Soc., London* **1964**, *84*, 845.

the protons 6 and 8, in agreement with the shorter distances that they have with their corresponding iron atoms 3 and 4. Similarly, the protons 1 and 3, which are the closest to their respective irons 1 and 2, have also greater anisotropic tensors than respectively those of the protons 2 and 4. These results indicate that, for each proton, the contribution coming from its closest iron plays the dominant role due to the r^{-3} law governing these anisotropic hyperfine interactions.

The third important feature apparent in Table I concerns the isotropic hyperfine couplings. If we consider the protons 5, 6, 7, and 8, we observe that the protons 6 and 8, which have the greatest isotropic couplings, are those which have the smallest anisotropic tensors. But the most striking feature is that the four protons 5, 6, 7, and 8, which are close to the mixed-valence pair, have all positive isotropic couplings. By contrast, the four 1, 2, 3, and 4 protons, which are close to the pair of ferric atoms have, negative isotropic couplings. These results will be analyzed in detail in Section V-1.

(IV) Determination of the Distribution of the Spin Population by Analysis of the Anisotropic Part of the Tensors

(1) Definitions. Let us first recall the meaning of the expressions "spin density" and "spin population", which are discussed in the following, since the expression "spin density" is often a source of ambiguities in the literature. In its proper meaning, the spin density is a local function $\rho^S(\vec{r})$ corresponding, at position $\vec{r}$, to the excess of spin up (or spin α) density over spin down (or spin β) density.[32a]

$$\rho^S(\vec{r}) = \rho^\alpha(\vec{r}) - \rho^\beta(\vec{r}) \qquad (5)$$

When the Fermi contact hyperfine interaction is considered, then the expression "spin density" designates the same quantity, but at the position of the nucleus N, i.e. $\rho^S(\vec{r}_N)$. However, in the context of molecular orbital descriptions, the same term of "spin density" is often attributed to another concept which is the fractional number of unpaired electrons $D_S(N)$ in an atomic orbital of the atom N.[33] In this last case it is much better to use the expression "spin population", since $D_S(N)$ is a scalar and not a function. If we come now to the analysis of the anisotropic parts of hyperfine tensors, we have to deal primarily with the spin density function $\rho^S(\vec{r})$. But, especially if we treat these quantities in the framework of the point-dipole approximation, it turns out that the $D_S(N)$ numbers become quite useful. Consequently, in order to avoid ambiguities, *these numbers will be called spin populations in the following.*

Coming to the paramagnetic center studied here, the fact that its resultant spin is $^1/_2$ means that the integration over the whole space of the associated spin density $\rho^S(\vec{r})$ is equal to 1. If this spin density is now considered within the point-dipole approximation, it is then redistributed on the different atoms N of the molecule under the form of a scalar $D_S(N)$ related to each atom. Under this condition, the sum of these scalars must then be close to 1. But it will not necessarily be exactly equal to it, due to the neglect of the small spin populations of the carbon and hydrogen atoms of the ligands.

Then, the (k,l) element of the tensor corresponding to the dipolar interaction between the nuclear spin I on the proton i and the spin density distribution characterized by the spin density function $\rho^S(\vec{r})$ can be written

$$T_{calc}{}^i(k,l) = g_e\beta_e g_I\beta_I \int (3x_k^i x_i^i - r_i^2) r_i^{-5} \rho^S(\vec{r})\, d\vec{r} \qquad (6)$$

In this expression, $\rho^S(\vec{r})$ corresponds to the normalized distribution of the spin density in the whole cluster and $\vec{r}_i$ is the vector from nucleus i to the point $\vec{r}$ at which $\rho^S(\vec{r})$ is evaluated. Here, $\rho^S(\vec{r})$ is equal to the $D_S(aa|r_1)$ term defined in the book of McWeeny and Sutcliffe.[32b] Since the point-dipole approximation is used in the following, this expression will be further simplified by assuming that $\rho^S(\vec{r})$ is approximated by a sum of Dirac functions centered on each nucleus i, these different functions being weighted by their corresponding spin populations $D_S(i)$.

(2) Validity and Use of the Point-Dipole Approximation. In the process of determination of these electron spin populations on the iron and sulfur atoms, we have, at first, attributed hypothetical spin populations to the different atoms of the cluster bearing a non-negligible fraction of the spin population. Then we have calculated "theoretical" anisotropic proton hyperfine tensors with these initial values, which have then been compared in an iterative process to the experimental ones in order to minimize their differences. Practically, only those of the protons 1, 3, 4, 5, 6, 7, and 8 have been used for this purpose by reason of the uncertainties, explained above, about the exactness of the values concerning the proton 2. Let us now discuss the validity of the approximations made during these calculations.

The first issue concerns the validity of the point-dipole approximation. It was tested by comparing the anisotropic hyperfine interaction calculated from the point-dipole approximation with the same interaction obtained from more rigorous calculations on an iron atom. This comparison has been made in the most drastic case, i.e. between the iron 3 and the proton 5, which corresponds to the shortest distance existing here between proton and iron atoms. A fictitious spin population of 1 has been placed on the iron 3, and the $3d_{z^2}$, $3d_{xy}$, $3d_{yz}$, $3d_{xz}$, and $3d_{x^2-y^2}$ Watson orbital wave functions[34] were successively used for the exact calculations. These comparisons show that the point-dipole approximation is already quite good for the distance considered. In effect, if we consider the principal value associated with the direction joining the two atoms (also taken here as the z direction of the orbitals), the value given by the point-dipole approximation deviates by −7% when compared to the values calculated with the $3d_{z^2}$ and $3d_{x^2-y^2}$ orbitals, which the error is −2% for those made with the $3d_{yz}$ and $3d_{xz}$ orbitals and +7% with the one made with the $3d_{xy}$ orbital. Since the five 3d orbitals are involved in our real problem, the errors due to the point-dipole approximation will mutually compensate, at least partially. Thus, in the case of the iron 3 and the proton 5, the error is in fact much less than 7%. Then, in the other cases where the iron–proton distance is greater, the point-dipole approximation is even much better. Similar calculations made for the interaction between the protons closest to the inorganic S^* atoms of the cubanes and the 3p orbitals of these atoms show that this hypothesis remains rather good. However, we must recognize that this hypothesis becomes rather coarse in the case of spin populations present on the sulfur atoms of the benzyl thiolate ligands. But we will see in the following that these imperfections are not very important because the spin populations are localized mainly on the four magnetic iron atoms, only small parts of them being distributed on the two kinds of sulfur atoms. Finally, the spin populations on the carbon atoms and hydrogen atoms of the CH_2 groups have been neglected, since they are expected to be less than the spin populations on their vicinal sulfur atoms.

However, a second problem must also be discussed before using the point-dipole approximation. It relies on the fact that the anisotropic part of the hyperfine interaction is due, for paramagnetic metal complexes, to two contributions while only one is generally considered for free radicals.[35] The first contribution is the classical "spin-only" dipolar interaction between the electron spin and the nuclear spin. But, there is another dipolar term

(32) McWeeny, R.; Sutcliffe, B. T. *Methods of Molecular Quantum Mechanics*; Academic Press: London, 1969; (a) p 87, (b) p 222, (c) p 104.
(33) Carrington, A.; McLachlan, A. D. *Introduction to Magnetic Resonance*; Harper International: New York, 1967; p 81.
(34) (a) Watson, R. E. *Phys. Rev.* **1960**, *118*, 1036. (b) Watson, R. E. Technical Report Number 12; Solid-State and Molecular Theory Group, M.I.T.: Cambridge, MA, 1959.
(35) Atherton, N. M.; Horsewill, A. J. *J. Chem. Soc., Faraday Trans. 1* **1980**, *76*, 660.

which is associated with the orbital magnetic momentum and which must be considered in metal complexes where the orbit is very often less quenched than in free radicals. The relative importance of these two contributions for the ligand hyperfine interactions in metal complexes has been discussed in particular by Marshall,[36] Atherton and Horsewill,[35] and Keijzers and de Boer.[37] For a complex of a paramagnetic metal and a nucleus of spin I in one of its ligands, the principal term due to the electron orbital momentum in the spin Hamiltonian is, at a first order of approximation

$$H = (\gamma\mu_B R^{-3})(3I_R L_R - \vec{I}\cdot\vec{L}) \quad (7)$$

where R refers to the metal to ligand nucleus direction and R is the distance between them. In practice, this term is proportional to R^{-3} and to a tensorial term corresponding to the difference between the **g** tensor and g_e. If R is small this term can be large, as is the case for a hyperfine interaction with the spin of the metal itself. But we want to show that this orbital contribution is negligible for the CH_2 protons due to the distances considered and also because the principal values of the **g** tensor do not differ largely from g_e. We have neglected the fact that the **g** tensors and the hyperfine tensors do not have parallel axes, since we only need to obtain an estimation of the maximal values of these orbital contributions with respect to the spin-only ones. Here, the values of R range from 2.98 Å, for the shortest distance between the iron 3 and the proton 5, to 6.70 Å, for the distance between the iron 1 and the proton 8. In order to evaluate the **g** tensor deviations $(\Delta g_1)_{ij}$, $(\Delta g_2)_{ij}$, $(\Delta g_3)_{ij}$, and $(\Delta g_4)_{ij}$ from g_e, which are relative to each individual iron 1, 2, 3, and 4, we have used the following expression[38]

$$(\Delta g)_{ij} = -{}^4/_3(\Delta g_1)_{ij} - {}^4/_3(\Delta g_2)_{ij} + {}^{11}/_6(\Delta g_3)_{ij} + {}^{11}/_6(\Delta g_4)_{ij} \quad (8)$$

where the $(\Delta g)_{ij}$ values correspond to the whole cluster in which the iron spins are already coupled. We have made these calculations, here again, in the case of the iron 3 and the proton 5 where R is minimum, in order to evaluate the maximum amount that the orbital contribution can attain with respect to the spin-only one. Moreover, since this iron belongs to the mixed-valence pair, it is expected to have much greater $(\Delta g_3)_{ij}$ deviations than those of the "ferric" irons 1 and 2. The upper limit reached by the orbital contribution is in this case 0.3 Mhz, which represents a maximum of 3% of the spin-only dipolar contribution to the anisotropic tensor. Since the orbital contributions of the other protons must be much weaker, all these orbital contributions can be taken as negligible.

A similar discussion has already been made in the case of the ENDOR study of the $Cu(H_2O)_6^{2+}$ complex by Atherton and Horsewill.[35,39] In this copper complex, these authors have estimated that the orbital contributions could represent, depending on the protons considered, between 7 and 15% of their total anisotropic proton tensors. These orbital contributions are more important in the copper complex than in our case for two reasons: their **g** tensor deviates about seven times more from g_e than the **g** tensor of our $[Fe_4S_4]^{3+}$ center and their distances between the protons and the copper atom are between 2.7 and 2.9 Å.[39]

In summary, the evaluations made above lead us to consider that the point-dipole approximation is valid for the treatment of our problem and that the spin-only term is, to a very good approximation, the only one determining the hyperfine interactions with the protons considered. But our final test at the practical level concerning the calculations of the anisotropic parts of these hyperfine interactions will be the ability of the model thus defined to give calculated anisotropic tensors which reproduce in a satisfying way the experimental ones.

Within these approximations, each calculated hyperfine tensor $T_{calc}{}^i$ for a defined proton i is approximated by a sum—over all the N iron and sulfur atoms under consideration—of component tensors $T^i(N)$ corresponding to the interaction with the atom N, each of the components being weighted by the corresponding spin population $D_S(N)$:

$$T_{calc}{}^i = \sum_{i=1}^{N} D_S(N)T^i(N) \quad (9)$$

Each tensor $T^i(N)$ is defined as follows: for the proton i and one single electron placed at the position R_i of the nucleus of the atom N, the principal values of the tensor $T^i(N)$ are

$$T_1 = 2g_e\beta_e g_I\beta_I R_i^{-3} = 158.12R_i^{-3} \quad \text{and} \quad T_2 = T_3 = -T_1/2 \quad (10)$$

where the distance R_i between the proton i and the electron is expressed in Å, while the principal tensor values are expressed in MHz. This tensor is axial, the principal direction associated with the principal value T_1 being the proton–nucleus direction.

In the approach followed here, our objective is to determine the spin population numbers $D_S(N)$ on the different iron and sulfur atoms. These numbers must, in fact, correspond to the sum of the populations of unpaired electrons which would have been assigned in a more rigorous model to the different atomic orbitals centered on the atom N involving these unpaired electrons.

In order to obtain the best possible set of values of $D_S(N)$, an iteration procedure is adopted which minimizes the differences between our experimental proton hyperfine tensors and the "theoretical" tensors calculated within the point-dipole approximation. More precisely, it minimizes the following error function erf depending on the spin populations placed on the different atoms:

$$\text{erf} = \sum_{i=1\ \text{but}\ i\neq 2}^{8} \sum_{j=1}^{3} \sum_{k=j}^{3} \left[\frac{T_{exp}{}^i(j,k) - T_{calc}{}^i(j,k)}{T_1(i)} \right]^2 \quad (11)$$

where i runs on the number of proton tensors considered and (j,k) runs on the number of tensor elements considered. The tensor of the proton 2 has not been involved in the minimization procedure since it is uncertain. The denominators $T_1(i)$ are chosen in each case as the greatest of the principal values of the experimental tensor $T_{exp}{}^i$. This procedure has been applied before diagonalization to the tensors $T_{exp}{}^i$, $T_{calc}{}^i$, and $T^i(N)$ defined in the (a, b, c^*) reference frame in order that the refinement might operate as well on the principal values as on the principal directions of the calculated tensors. Since the error function is a sum of quadratic functions with respect to the parameters $D_S(N)$ that we want to obtain, the convergence toward a unique minimum is certain.

The final tensors are reported in Table II, where they are compared to the experimental ones. The agreement between the experimental and calculated results is quite good, and particularly for the protons 5, 6, 7, and 8, which are on the side of the mixed-valence pair of iron atoms. The contribution of these four protons to the value of the error function (11) is only 11%; this indicates that the model simulates their tensors better than those of the protons 1, 3, and 4.[40] Concerning the principal directions, the mean difference between calculated and experimental tensors is 6° for the protons 5, 6, 7, and 8 while it is 14° for the protons 1, 3, and 4.

The differences remaining between our experimental results and those given by the model and also the difference in quality of the tensors calculated for the protons 5, 6, 7, and 8 compared to those calculated for the protons 1, 3, and 4 can have two different possible origins:

The first one can be associated with the imperfections of the point-dipole model. As we have seen above, these errors are negligible due to the distances involved for the dipolar interactions

(36) Marshall, W. In *Paramagnetic Resonance*; Low, W., Ed.; Academic Press: New York, 1963; p 347.
(37) Keijzers, C. P.; de Boer, E. *J. Chem. Phys.* **1972**, *57*, 1277.
(38) Noodleman, L. *Inorg. Chem.* **1988**, *27*, 3677.
(39) Atherton, N. M.; Horsewill, A. J. *Mol. Phys.* **1979**, *37*, 1349.

(40) The tensor of the proton 2 is not considered in these comparisons since it has been reconstituted essentially with the help of the point-dipole model.

Table II. Comparisons of the Anisotropic Parts of the Hyperfine Tensors Obtained Experimentally with Those Calculated with the Point-Dipole Model[a]

protons	anisotropic tensor: experimental values	anisotropic tensor: calculated values	angular deviations[b] (deg)
	−2.64	−2.45	15
1	+2.19	+1.88	14
	+0.45	+0.57	17
	−2.34	−1.99	12
3	+2.03	+1.69	9
	+0.31	+0.30	10
	−0.92	−0.95	16
4	+0.83	+0.70	14
	+0.09	+0.24	10
	+8.71	+8.49	5
5	−6.27	−5.56	5
	−2.44	−2.92	6
	+4.25	+4.12	5
6	−2.35	−2.41	4
	−1.90	−1.71	3
	+7.00	+7.55	5
7	−4.95	−4.77	5
	−2.05	−2.89	4
	+3.35	+3.61	1
8	−1.95	−2.05	17
	−1.40	−1.56	17

[a] The calculated values correspond to the final step 4 of our refinement procedure (see Table III). Note that the tensor of proton 2 has not been taken into account here, for the reason given in the text and in the caption of Table I. [b] For each principal value of each proton tensor, the angular deviations given in the last column correspond to the angle found between the calculated principal direction and its corresponding experimental principal direction.

involving the iron atoms. The same argument of distance also remains valid for the contributions of the spin populations lying on the S* atoms of the cluster, in spite of the fact that the sulfur 3p orbitals are more diffuse and long range than the 3d orbitals of the irons. But this approximation becomes very crude for the spin populations on the S atoms of the benzyl thiolate ligands, these sulfurs being closer to the protons of the CH_2 groups than the inorganic ones. Since the dipolar tensors of the protons 1–4 are small, this imperfection must have greater consequences for the S* atoms placed on the side of the ferric pair. In effect, the contributions coming from the S* atom of the benzyl thiolate ligands bound to the irons 1 and 2 are expected to be comparatively greater for these protons and their uncertainties will have a greater effect on these tensors than on those of the protons 5–8. But, anyway, these errors are not of major importance, since we will see that the spin populations on these sulfurs are small.

The second kind of imperfections able to explain differences between calculated and experimental values is associated with uncertainties in the distances between the protons and the atoms bearing the unpaired-spin populations. We have used without modification the distances taken from the X-ray structure of the crystal in these calculations.[28] However, these distances are not exactly those, unknown to us, that, in principle, we would have to use in these calculations. The first reason for this discrepancy is that the X-ray structure has been determined at room temperature[28] while our ENDOR experiments are run at 10 K. Due to the expansion of the unit cell between 10 and 300 K, the distances that we use are somewhat overestimated. This discrepancy can be estimated with the help of the study of a phase transition made in a similar compound: $[Bu_4N]_2[Fe_4S_4(SC_6H_5)_4]$.[41] In this compound, the unit-cell dimensions of crystals have been measured as a function of temperature around the phase transition, i.e. between 175 and 290 K. These variations are anisotropic, but on the average, their relative slope $\Delta L/L$ is 9×10^{-5} per degree. Assuming a quadratic law for the crystal

(41) Excoffon, P.; Laugier, J.; Lamotte, B. *Inorg. Chem.* **1991**, *30*, 3075.

Table III. Values of the Spin Populations D_S Obtained on the Different Iron and Sulfur Atoms for the Center IV[a]

atoms	step 1	step 2	step 3	step 4
Fe_1	−0.730	−0.711	−0.711	−0.722
Fe_2	−0.730	−0.739	−0.739	−0.618
Fe_3	+1.370	+1.288	+1.288	+1.293
Fe_4	+1.370	+1.452	+1.452	+1.359
S^*_1 and S^*_2			0.000	0.000
S^*_3 and S^*_4			0.000	0.000
S_5				−0.056
S_6				−0.048
S_7				+0.037
S_8				+0.039
total spin population	+1.280	+1.290	+1.290	+1.284
error function erf	1.195	1.173	1.173	0.612

[a] These values were obtained at the issue of the four successive steps of refinement of the minimization procedure described in the text. Following the usual conventions, the atoms designated by S* correspond to the inorganic sulfurs of the cubane and those designated by S are those of the benzyl thiol ligands. The labeling of the atoms is taken from the X-ray structure.[28]

expansion as a function of temperature between 10 and 300 K, we can estimate to about 2% the mean relative change in the dimensions of the unit cell of this crystal between these two temperatures. We can make the hypothesis that the changes of the iron–proton distances in the crystal studied here between 300 and 10 K are of the same order or less.[42] But a second problem must be considered concerning the distances which must be used here with the point-dipole model: in effect, we deal here with a $[Fe_4S_4]^{3+}$ species created by irradiation in this crystal while the distances taken from the crystallographic structure are relative to the original $[Fe_4S_4]^{2+}$ clusters. Small changes in the distances are expected between the two, since the increased positive charge on the cubane structure can slightly decrease the iron–proton distances. We can add that these changes might be relatively more important on the side of the irons 1 and 2 than on the side of the irons 3 and 4. In effect, roughly, γ irradiation changes the first two irons from mixed-valency to ferric while the last two ones remain unchanged. This eventuality is somewhat substantiated by our results reported in Table II, indicating that the greatest contributions to the error function (11) are due to the protons 1, 3, and 4. But we think that, anyway, all these changes in the iron–proton distances are small, since they must be limited by the intricacy of the molecular stacking with the surrounding counterions and complexes in the crystal.

In summary, the two causes of uncertainty in the distances discussed above must be small and their effects are probably in opposite directions. Thus, it is probably a good approximation to neglect them. Consequently, we estimate that the capacity to reproduce with good precision the experimental proton hyperfine tensors by calculations based on the atomic positions of the X-ray structure will be the best indication that the changes discussed above must be of minor importance.

(3) Results: Distribution of the Spin Populations. The spin populations $D_S(N)$ thus obtained are presented in Table III. They have been obtained in a refinement procedure involving four successive steps, by increasing at each step the number of independent spin populations to be determined. In the first step (Step 1 in Table III), we have only considered the spin populations placed on two pairs of iron atoms, the iron atoms in each pair being equivalent between them at this stage. In the second step (Step 2), we have considered the possible occurrence of spin populations at the level of the four S* atoms of the cluster. They are treated as two different pairs, with equivalent sulfur atoms

(42) This transposition supposes that the intramolecular distances have similar variations as the unit-cell dimensions and also that the two compounds have roughly, on the average, the same variations of the unit-cell dimensions with temperature. Since the compound studied in ref 41 exhibits important effects due to the mobility of the butyl end groups, we suspect that the estimation made with its help gives us a maximum value.

in each pair. The possibility of inequivalence between iron atoms in each pair is introduced in the third step. At last, the possible occurrence of spin populations at the level of the four S atoms of the benzyl thiolate ligands is introduced in the fourth step. The spin populations obtained after minimization of the error function (11) at the end of this fourth step constitute our final results. We can make the following observations on their values:

(i) The spin populations obtained on the iron atoms 3 and 4 have the same positive signs; this is the indication of ferromagnetic order between the spins on these two atoms. This result agrees with the fact that these two atoms belong to the "mixed-valence pair" for which ferromagnetic order prevails, due to the electron delocalization[43] in this pair.

(ii) The negative vs positive signs of the spin populations on the iron atoms 1 and 2 with respect to the iron atoms 3 and 4 indicate that the spin populations on the "ferric pair" and on the "mixed-valence pair" are in antiferromagnetic order between them. This is consistent with the fact that the exchange terms chosen to describe the magnetic properties of the iron–sulfur clusters are antiferromagnetic.[44]

(iii) The irons 1 and 2 (crudely considered as Fe^{3+} ions) have spin populations of the same sign. This is an indication of a predominant ferromagnetic order between them, in apparent contradiction with the antiferromagnetic character of the exchange terms involved, as discussed above. Its origin is certainly related to the situation of *frustration* (with respect to antiferromagnetic ordering) imposed by the tetrahedral topology of the four iron atoms which continues to exist even if the delocalization in the mixed-valence pair imposes ferromagnetic order between its irons spins. This problem will be discussed in more detail in Section IV-7.

(iv) We find that the spin populations on the irons 1 and 2 are not equal, but not very different. The same observation can be made for those of the irons 3 and 4 of the mixed-valence pair. These results could be expected, since the Fe_4S_4 cubane does not possess any true symmetry element in the crystal.[28]

(v) By contrast with those on the iron atoms, the spin populations obtained on the sulfur atoms are weak. Their values must be considered as only approximate, since the point-dipole approximation is less valid for the sulfurs, especially those of the thiolates. We have found weak values for the spin populations on the sulfurs of the thiolate ligands which have the same sign as those on their adjacent iron atom. But we find zero values for the four inorganic sulfurs of the cluster. The fact that the spin populations on the inorganic sulfurs are weaker than those on the sulfurs of the thiolate ligands can be due to limitations of the model used and (or) to cancelation effects. It is in effect reasonable to make the supposition that—at the level of each sulfur atom of the cubane—the positive spin populations transmitted from their vicinal Fe_3 and Fe_4 atoms are reduced by the negative spin populations transmitted from their vicinal Fe_1 and Fe_2 atoms.

(vi) In principle, the spin population numbers $D_S(N)$ correspond to a distribution which is normalized to 1. The sum (1.28) of the spin populations that we obtain on the four iron atoms is not far from but somewhat greater than 1. The difference between these two numbers originates in some part from the fractions of the spin population distributed on all the other atoms of the cluster and the ligands. The remaining part must come from the uncertainties attached to the spin populations on the sulfur atoms and also from the superposition of the different types of errors discussed in the previous paragraphs.

(4) Meaning of the Spin Population Numbers Obtained. In order to appreciate correctly the meaning of the results obtained in Table III, it is now useful to make some more general considerations. This study is in fact at the crossroads of two different areas of research activity: (a) the studies of spin density (or, better said, of spin population) distributions in paramagnetic molecules based on ENDOR spectroscopy in single crystals which, more often, have been performed in free radicals and sometimes in monometallic complexes but which, to our knowledge, have never been undertaken in such polymetallic systems. (b) the studies of the hyperfine interactions in paramagnetic iron–sulfur clusters which, up to now, have been essentially discussed on the basis of Mössbauer studies.

Our aim is to perform in these polymetallic complexes what has been done in the past for radicals or monometallic complexes. But since the procedures and concepts used in these two domains generally differ (people familiar with one being often less familiar with the other), we find it useful, for clarity, to set explicitly these two approaches and to discuss their relations and differences.

Examples of detailed proton ENDOR studies can be found for free radicals,[45] phosphorescent triplet states of aromatic molecules,[46] and simple transition metal complexes.[35,47] However, the system treated here is more complex than these previous ones, since it corresponds to a polymetallic cluster where, in principle, nineteen unpaired electrons must be considered and where, moreover, the electron spin population is delocalized on several metallic and ligand atoms.

Let us compare the distribution of the spin population obtained here with the ones characteristic of the $S = {}^1/_2$ delocalized aromatic free radicals. In these radicals, the "fractional" spin populations $D_S(i)$ on the different C_i carbon atoms are always lower (and generally much lower) than 1. This is easily understood in the framework of molecular orbital descriptions in which they can be represented, in a good approximation, by a single unpaired electron occupying their highest occupied molecular orbital. Then, these spin populations roughly represent the fraction of the unpaired electron present in each carbon $2p_z$ orbital. Generally, their $D_S(i)$ values are positive, except for the odd-alternant aromatic hydrocarbon ions where small negative values are found for particular carbon atoms. These "negative spin densities" correspond to an antiferromagnetic order of the magnetization on these atoms with respect to the one on their neighbor carbon atoms. They can only be understood within the framework of an unrestricted molecular orbital description which considers that the spin densities on the different carbon atoms result from the difference between the α spin and β spin densities. In these cases of odd-alternant aromatic radicals, at least two different molecular orbitals must be involved to describe the magnetic properties of these molecules and the pleasant but oversimplified representation of the system as containing a unique unpaired electron must then be forsaken.

In the present study of this $[Fe_4S_4]^{3+}$ species which has also a resulting spin expectation value of $S = {}^1/_2$, we find that the absolute values of the spin populations on the iron atoms are much larger than those found in the delocalized free radicals. The positive spin populations corresponding to the Fe_3 and Fe_4 atoms of the mixed-valence pair are greater than 1, while the two others are negative but also rather large. The unrestricted representation of the electronic levels is essential in this problem, and the distribution of the spin population obtained must be considered as the result of the summation and partial annihilation, at the level of each iron atom, of the numerous subjacent α and β monoelectronic level populations distributed principally in different 3d orbitals (but also in 3p orbitals) resulting in net α spin population on the irons 3 and 4 and net β spin population on the irons 1 and 2. The differences existing between the cluster

(43) (a) Zener, C. *Phys. Rev.* **1951**, *82*, 403. (b) Anderson, P.; Hasegawa, H. *Phys. Rev.* **1955**, *100*, 675.

(44) Papaefthymiou, G. C.; Laskowski, E. J.; Frota-Pessôa, S.; Frankel, R. B.; Holm, R. H. *Inorg. Chem.* **1982**, *21*, 1723.

(45) (a) Lamotte, B.; Gloux, P. *J. Chem. Phys.* **1973**, *59*, 3365. (b) Gloux, P.; Lamotte, B. *Mol. Phys.* **1972**, *24*, 23; **1973**, *25*, 161.

(46) Hutchison, C. A., Jr.; Kohler, B. E. *J. Chem. Phys.* **1969**, *51*, 3327.

(47) (a) Hutchison, C. A., Jr.; McKay, D. B. *J. Chem. Phys.* **1977**, *66*, 3311. (b) Balmer, P.; Blum, H.; Forster, M.; Schweiger, A.; Günthard, H. H. *J. Phys. C: Solid State Phys.* **1980**, *13*, 517. (c) Brown, T. G.; Hoffmann, B. M. *Mol. Phys.* **1980**, *39*, 1073. (d) Rudin, M.; Schweiger, A.; Günthard, H. H. *Mol. Phys.* **1982**, *46*, 1027.

studied here and the radicals are the result of the much greater number of unpaired electrons involved in the iron–sulfur clusters. They are also due to the differences in energy between their electronic levels, which are also much weaker than those for the radicals, the bonds between the iron and sulfur atoms in the clusters being also much weaker than the covalent bonds in the radicals.

By contrast with the radicals generally discussed in terms of molecular orbital LCAO descriptions, the practice, up to now, of Mössbauer and EPR experimentalists in the domain of the iron–sulfur clusters has been to discuss their magnetic properties within the framework of the simplistic, pure valence-bond, description, which neglects the delocalization of the spins on the sulfur (and other) atoms.[48] These descriptions are based on four high-spin-state iron atoms ($S = 2$ for Fe^{2+} and $S = {}^5/_2$ for Fe^{3+}) which are magnetically coupled with a vector model. In spite of the fact that we are dealing here with more detailed results involving delocalization on the sulfur atoms, in practice, we have thus the obligation to analyze the results contained in Table III within the terms of this simplifying model in order to relate them to the analyses made in the previous Mössbauer studies of the $[Fe_4S_4]^{3+}$ state.[9-11]

(5) Some Recollections Concerning Analyses of the ^{57}Fe Hyperfine Interactions. Before our recent ^{57}Fe ENDOR single-crystal study[3] of the paramagnetic center studied here by proton ENDOR, the ^{57}Fe hyperfine tensors corresponding to the $[Fe_4S_4]^{3+}$ state had been measured by Mössbauer methods, first in the oxidized state of the high-potential protein from *Chromatium*[9,10] and, more recently, in the $(NBu_4)[Fe_4S_4(S\text{-}2,4,6\text{-}(i\text{-}Pr)_3C_6H_2)_4]$ synthetic analogue.[11] These results have been discussed in terms of a spin-coupling model involving a Fe^{3+}–Fe^{3+} pair and a delocalized Fe^{2+}–Fe^{3+} pair. The validity of this model has been checked by the ability to elaborate a spin-coupling scheme to reproduce the isotropic parts of the hyperfine A_{Fe} tensors from the corresponding values $a(Fe^{2+})$ and $a(Fe^{3+})$ associated with monomeric irons with tetrahedral sulfur coordination. The values of $a(Fe^{2+}) = -22$ Mhz and $a(Fe^{3+}) = -20$ Mhz corresponding to the isotropic ^{57}Fe couplings of the rubredoxin protein have been chosen in practice as the basic monomeric values.[49]

In the discussions of the Mössbauer results on the iron–sulfur clusters, the measured A_{Fe} values which do correspond to the *coupled system* of iron atoms and are related to the spin of the whole center are distinguished from the $a(Fe^{2+})$ and $a(Fe^{3+})$ defined above, which are considered for their part as "related to their individual spins",[10] *before magnetic coupling*. The last ones are the "*local site*" *values* at the level of each iron atom, and they constitute the building blocks of the pure valence-bond model in which the spins on the individual iron atoms are subsequently vectorially coupled. The vector-coupling coefficients K_i relate the first values to the last ones by the expression

$$A_i = K_i a_i \tag{12}$$

where the index i refers to the different iron atoms. These coefficients K_i are calculated by two successive applications of the Wigner–Eckart theorem. At first, the two spins of the iron atoms of the mixed-valence pair are coupled together to give a resulting spin S_{m-v}, while the two spins of the ferric atoms are also coupled to give the resulting spin S_{ferric}. Then, S_{m-v} and S_{ferric} are subsequently coupled to give the resulting spin state S_{total}. Thus, in this model, the magnetic state of the cluster is described by the ket $|S_{m-v}, S_{ferric}, S_{total}\rangle$.[38] At first glance, it seemed that the state $|{}^9/_2,5,{}^1/_2\rangle$ might be proposed to represent the magnetic ground state of the $[Fe_4S_4]^{3+}$ cluster. But this hypothesis had to be discarded because it would have given positive ^{57}Fe hyperfine couplings for the irons of the mixed-valence pair and negative ones for those of the ferric pair,[38] just in opposition to the experimental results.[9-11] This state would have also given an average value of the **g** tensor inferior to the free-electron value, in opposition to the experimental results.[7,11] Then, Noodleman showed[38] that, instead, the $|{}^9/_2,4,{}^1/_2\rangle$ spin state would correspond to the ground state, since it predicts $A_{m-v} = -38.5$ Mhz and $A_{ferric} = +26.7$ Mhz. The experimental values to which these calculated values must be compared are $A_{m-v} = -30$ and -32 Mhz for respectively the protein[10] and the synthetic model[11] and $A_{ferric} = +20$ Mhz for the protein and the synthetic model.[10,11] Moreover, the $|{}^9/_2,4,{}^1/_2\rangle$ state predicts a value of $g_{av} = 2.08$, which is also in rather good agreement with the experiments; it is certainly much better than the value smaller than 2 that the $|{}^9/_2,5,{}^1/_2\rangle$ state predicts.

But, we have also to consider more recent information which has been obtained on this subject. In effect, the temperature dependence of the magnetic susceptibility of the model compound $[Fe_4S_4(S\text{-}2,4,6\text{-}(i\text{-}Pr)_3C_6H_2)_4]^-$ has been successfully fitted between 5 and 320 K. It indicates that two excited magnetic levels must be taken into account, since they are relatively close to the fundamental state. The result, in this particular model compound, is that the level of the $|{}^7/_2,3,{}^1/_2\rangle$ state is only at 11 cm^{-1} above the fundamental state, while the $|{}^5/_2,2,{}^1/_2\rangle$ state is at 167 cm^{-1} above it.[50] We estimate that the positions of these state levels are likely to vary appreciably for clusters in the same oxidation state, but with varied ligands. Anyway, this result suggests at least that the level of either the $|{}^9/_2,4,{}^1/_2\rangle$ state or the $|{}^7/_2,3,{}^1/_2\rangle$ one can be a candidate to represent the fundamental state, since they are nearly degenerate in the case of the $[Fe_4S_4(S,2,4,6\text{-}(i\text{-}Pr)_3C_6H_2)_4]^-$ model compound. Thus, it is likely that either one or the other of the above states could correspond to the fundamental spin state of the $[Fe_4S_4]^{3+}$ cluster, depending on small changes of geometry of the cubane itself and depending also on the nature and the conformations of the ligands.

Our purpose in the following paragraph will be to discuss the spin populations of Table III in light of the model discussed above, being however aware of its rather stringent limits. As we will see, this approach will lead us to put forward a new proposal for the fundamental $[Fe_4S_4]^{3+}$ spin state in center IV that we estimate also relevant to the interpretation of the previous Mössbauer and NMR results in the protein and the model compound.

(6) Analysis of Results in Terms of "Local Site" Iron Spin Populations. The idea that we follow here is to transpose the approach relative to the ^{57}Fe isotropic hyperfine couplings into a similar one concerning the spin populations. Following the spirit of this model, we connect—through the K_i coefficients—the fractions D_S of the spin population of spin ${}^1/_2$, *related to the whole center* that we measure, to the P_{vml} spin populations, *defined as related to the local total spin assigned to each iron atom, before magnetic coupling*. These populations are called here P_{vml} for "vector-model local spin populations", in order to contrast them from the $D_S(i)$ of Table III. They correspond to the difference between the population of the spin α electrons and the spin β electrons[32c] on each uncoupled iron atom. Then, these two quantities are related by the expression

$$P_{vml}(i) = 2S_i[D_S(i)/K_i] \tag{13}$$

where S_i is the total spin number related to each iron atom and $2S_i$ is the number of 3d unpaired electrons attached to each magnetically isolated iron atom.

In the simplistic pure valence-bond model, the total spin population of the cluster is entirely localized on the magnetic iron

(48) We do not allude here to first-principles functional density Xα calculations made in other respects by theoreticians on the iron–sulfur clusters family (see in particular ref 51 and references therein), for which further comparisons of their predictions with our experimental results will be interesting to do in order to analyze these results at a deeper level.

(49) Papaefthymiou, V.; Girerd, J. J.; Moura, I.; Moura, J. J. G.; Münck, E. *J. Am. Chem. Soc.* **1987**, *109*, 4703. Münck, E.; Papaefthymiou, V.; Surerus, K. K.; Girerd, J. J. In *Metals in Proteins*; Que, L., Ed.; ACS Symposium Series, No. 372; American Chemical Society: Washington, DC, 1988; p 302.

(50) Jordanov, J.; Roth, E. K. H.; Fries, P. H.; Noodleman, L. *Inorg. Chem.* **1990**, *29*, 4288.

atoms. Consequently, $P_{vml}(Fe^{2+}) = 4$, since four unpaired electrons are attached to a ferrous high-spin iron, and $P_{vml}(Fe^{3+}) = 5$, since five unpaired electrons are attached to a ferric high-spin iron. Then, $P_{vml}(i) = 2S_i$, and the expression 13 simply becomes

$$D_S(i) = K_i \tag{14}$$

This last expression means that the $D_S(i)$ are nothing else than the vector-coupling coefficients K_i when the simplistic approximation stating that the unpaired spin populations are only localized on the iron atoms is made.

It then follows that, within this approach, the assignment of our center IV to a given magnetic ground state can be obtained by *comparison* of the $D_S(Fe_i)$ values deduced from our experiments with the values of the coefficients K_i corresponding respectively to the $|^9/_2,4,^1/_2\rangle$, $|^7/_2,3,^1/_2\rangle$, and $|^5/_2,2,^1/_2\rangle$ spin states. But the reality is more complex than the representation given by this model, since our results indicate that spin populations are also present on the sulfur atoms of the ligands. This is why (following a somewhat paradoxical procedure!) *we are obliged to relocalize on the iron atoms* all the spin population present on the sulfur S and S* atoms, *in order to compare our experimental spin populations to the K_i coefficients*. This relocalization can be easily done for the spin populations on the S sulfurs of the benzyl thiolate ligands for which we have determined approximate values (see Table III). But we have difficulty for the inorganic sulfurs S*, because since each of them is bonded to three irons, the spin population that they bear must be the resultant of delocalizations coming from these three irons. For each of them, the problem is that it would be necessary to delineate the separate fractions of spin populations due to the delocalization originating from each iron which, in fact, add their effects at the level of each S* atom. We have found zero spin population on them (see Table III) and attributed this result to cancelation effects between the positive and negative contributions coming—for each S* atom—from its three adjacent iron atoms. But we have now to separate these three contributions without the help of any information as to how to perform them. However, in order to estimate the global amount of spin population that must be relocalized on each iron atom, we have adopted the only possibility remaining, which consists in taking four times the population on the corresponding sulfur of the benzyl thiolate ligand. This approximation is not too bad because, anyway, these spin populations on the sulfur atoms are much weaker than those on the iron atoms. We have obtained in this way new spin populations $D_S^*(i)$ on the four iron atoms that we compare directly to the K_i coefficients relate to the three spin states $|^9/_2,4,^1/_2\rangle$, $|^7/_2,3,^1/_2\rangle$, and $|^5/_2,2,^1/_2\rangle$. In the model under consideration, the two iron atoms are equivalent in the mixed-valence pair as well as in the ferric pair and we have only two values $K(Fe^{2.5+})$ and $K(Fe^{3+})$ to consider. This is why, for the sake of this comparison, we have averaged, in each of these pairs, the inequivalent spin populations $D_S^*(i)$ deduced from our experiments, thus giving $D_S^*(Fe^{2.5+}) = +1.48$ and $D_S^*(Fe^{3+}) = -0.88$. The values to which they must be compared are respectively $K(Fe^{2.5+}) = +1.83$ and $K(Fe^{3+}) = -1.33$ for the $|^9/_2,4,^1/_2\rangle$ state, $K(Fe^{2.5+}) = +1.50$ and $K(Fe^{3+}) = -1.00$ for the $|^7/_2,3,^1/_2\rangle$ state, and, at last, $K(Fe^{2.5+}) = +1.17$ and $K(Fe^{3+}) = -0.67$ for the $|^5/_2,2,^1/_2\rangle$ state.

Since *the $D_S^*(i)$ values deduced from our experiments are fairly close to the K_i coefficients of the $|^7/_2,3,^1/_2\rangle$ state* and they disagree with those corresponding to the two other states, *we must conclude that indeed the paramagnetic center that we study here must be identified with this state, within the limits of this crude model*. This conclusion is reinforced by the fact that the $D_S^*(i)$ values thus obtained are slightly weaker than the K_i values of the $|^7/_2,3,^1/_2\rangle$ state. This is in agreement with our estimation that the approach based on the point-dipole approximation somewhat underestimates the spin populations on the sulfur atoms. These considerations completely discard the possibility that our paramagnetic center could be represented by the $|^9/_2,4,^1/_2\rangle$ state. They might even reintroduce the possibility of the $|^5/_2,2,^1/_2\rangle$ state, if the spin populations on the sulfurs were much greater than we have supposed here.

Let us add that calculations on the $|^7/_2,3,^1/_2\rangle$ spin state similar to those made in ref 38 on the $|^9/_2,4,^1/_2\rangle$ state strongly support the attribution of the center IV to the $|^7/_2,3,^1/_2\rangle$ spin state. In effect, this $|^7/_2,3,^1/_2\rangle$ spin state predicts isotropic ^{57}Fe hyperfine couplings of −33.0 Mhz for the irons of the mixed-valence pair and of +20.0 Mhz for the irons of the ferric pair. These values are in excellent agreement with those that we measured by ^{57}Fe ENDOR on the same paramagnetic center: i.e. −33.5 and −32.7 Mhz for the two irons of the mixed-valence pair and +19.8 and +17.4 Mhz for those of the ferric pair.[3] This agreement is indeed much better than that with the values of respectively −38.5 and +26.7 Mhz (already cited in IV-5), that the model attributes to the $|^9/_2,4,^1/_2\rangle$ state.[38]

(7) Further Considerations Concerning the Valence-Bond and Vector Spin Coupling Models. (i) It is enticing to build for the $|^7/_2,3,^1/_2\rangle$ spin state a visual representation of the spin coupling scheme considering that the spins on each iron atom are simple vectors which are nothing else than the localized moments used by physicists in magnetism. The important fact is that, in this state, the expectation values of S_{m-v} and S_{ferric} are both smaller than their maximal possible values. *This means that the spin vectors on the different irons are not aligned but one is canted with respect to the others*. Thus, the obtention of $S_{m-v} = {}^7/_2$ instead of ${}^9/_2$ indicates that the spin vectors on the irons 3 and 4 are canted between them, while $S_{ferric} = 3$ instead of 5 implies that *the most important canting arises between the spin vectors of the two ferric irons 1 and 2*.

This situation is, in fact, the result of antagonistic magnetic interactions at work in the cluster combined with a topological situation of frustration. In effect, in the iron–sulfur clusters, all the exchange interaction terms J are considered to be antiferromagnetic. But since the four iron atoms are disposed in a tetrahedral topology, a situation of frustration is present for their spin vectors. In addition, the electronic delocalization in the mixed-valence pair tends to impose a ferromagnetic order to the spin vectors of this pair, this last effect being represented by the double-exchange term B.[38,43,49]

The relative orientations of the spin vectors in the $|^7/_2,3,^1/_2\rangle$ spin state thus represent the response of the spin system to these constraints and indicate how it finds *a compromise* to satisfy partially all of them. The greatest canting found between the spins of the two ferric irons is the indication that the effect of the frustration is maximum there. This observation is satisfying, since there must be no frustration between the iron spin vectors of the mixed-valence pair and also no more if each of them is taken separately with each of the two ferric spin vectors. We can even add that the canting existing between the iron spin vectors of the mixed-valence pair gives evidence that the electronic delocalization must be shared to some extent by the four iron atoms.

In spite of its qualitative character, this vectorial representation of the spin coupling scheme presents the interest to constitute a suggestive and useful picture of the magnetic properties of this $[Fe_4S_4]^{3+}$ cubane. But it must be used with caution, remaining aware that the description in terms of localized moments is an oversimplification for these delocalized clusters.

(ii) The functional density Xα calculations based on the use of broken symmetry wave functions[51] constitute a more fundamental way to treat these iron–sulfur clusters at the theoretical level than those based on phenomenological spin Hamiltonians. In these treatments, the electrons possess α or β spins of opposite directions, and the notion of spin vectors on individual atoms

(51) Noodleman, L.; Case, D. A. *Advances in Inorganic Chemistry*; Sykes, A. G., Ed.; Academic Press: San Diego, CA, 1992; Vol. 38, pp 423–470 and references contained therein.

Table IV. Proton Isotropic Hyperfine Couplings A^i_{iso} and Their Corresponding Values A^{*i}_{iso} Obtained after Normalization with the Help of the Expression 15 and the Spin Populations on the Irons Contained in Table III, Values of A^{*i}_{iso} Calculated by the Least Square Fit (see Figure 4), and Percentage of the Difference between the Normalized Experimental and Calculated Values (Note That, as in Table II and for the Same Reasons, the Tensor of Proton 2 Has Not Been Taken Into Account Here)

protons	1	3	4	5	6	7	8
A^i_{iso} (experimental values)	−1.95	−1.04	−2.00	+1.86	+3.63	+1.60	+2.60
A^{*i}_{iso} (normalized experimental values)	+2.70	+1.68	+3.24	+1.44	+2.81	+1.18	+1.91
A^{*i}_{iso} (normalized values deduced from the fit)	+2.82	+1.33	+2.75	+1.55	+2.89	+1.27	+1.99
deviation percentages	+4	−21	−15	+8	+3	+8	+4

with canting between them has no apparent basis. This proposition does not imply that the topological situation of spin frustration has vanished in these more rigorous representations. But, the problem of frustration is not apparent in this formalism. It is in fact hidden and reappears only when the results of the calculations made with the general electronic Hamiltonian must be reinterpreted in terms of Heisenberg-like spin Hamiltonians or, more precisely said, when the broken symmetry wave functions are expressed in terms of combinations of pure spin functions.[51]

We find it interesting to figure rapidly and qualitatively the results of Table III in light of these representations. Let us first consider the treatment given for the 2Fe–2S dimer.[52] The α spin density is then contained in orbitals essentially centered on one iron atom, while the β spin density is essentially centered on the other iron atom. Thus, roughly speaking, this dimer is composed of two clouds, one with α spin density on one iron and the other with β spin density on the other iron atom. These two clouds overlap, resulting in a decrease of the spin population numbers to values smaller than 4 or 5, which are the numbers that the pure valence-bond model attributes respectively to the Fe(II) and Fe(III) atoms. We can represent qualitatively, in a similar way, the $[Fe_4S_4]^{3+}$ cluster as constituted of two clouds between which there is spin separation.[53] Then, the first cloud, constituted of α spins, is centered on the two irons of the mixed-valence pair while the other, of β spins, is centered on the ferric pair. In practice, these two clouds overlap in a complicated way, resulting in values of the spin populations on each of the irons corresponding to the ones that we have determined in our experiments.

(iii) The assignment of the $[Fe_4S_4]^{3+}$ center IV to the $|^7/_2,3,^1/_2\rangle$ spin state has important consequences for the interpretation of the previous Mössbauer studies of the oxidized state of the *Chromatium* high-potential (HP) protein[9,10] and also of its $[Fe_4S_4(S\text{-}2,4,6\text{-}(i\text{-}Pr)_3C_6H_2)_4]^-$ model compound.[11] In effect, our values of the isotropic ^{57}Fe hyperfine couplings for this center IV[3] are almost identical to those measured by Mössbauer in this protein and model compound. *Consequently, we must conclude that the fundamental spin state of the Chromatium HP protein and of its* $[Fe_4S_4(S\text{-}2,4,6\text{-}(i\text{-}Pr)_3C_6H_2)_4]^-$ *model compound, whose knowledge is founded on these Mössbauer studies, has to be identified with the* $|^7/_2/3,^1/_2\rangle$ *spin state and not with the* $|^9/_2,4,^1/_2\rangle$ *one, as it was previously supposed.*

(V) Analysis of the Isotropic Part of the Proton Hyperfine Tensors: A Quantitative Model for the Interpretation of Paramagnetic Shifts of Protons in the NMR Spectra of the Iron–Sulfur Proteins

The analysis of the anisotropic parts of the tensors of Table I has been a fertile source of information on the magnetic structure of the $[Fe_4S_4]^{3+}$ state. But we have now to take advantage of their isotropic parts which represent another rich source of new information, useful to the interpretation of the paramagnetic shifts of the β-CH_2 protons of cysteines measured in recent NMR studies of the oxidized state of high-potential ferredoxins.[13-16,54]

In the following paragraphs, we will analyze the isotropic hyperfine couplings of the different protons and we will show that we can relate their values to the spin populations and the geometrical conformation of the ligands. We will proceed in a general way in this prospect, taking advantage of the knowledge of magnetic and geometrical nature that we have on our system. Consequently, we will avoid the, a priori, simplifying hypotheses generally used in the literature for the proton paramagnetic shifts which are used because of the lack of precise information such as those obtained here. Then, we will discuss the nature of the underlying mechanisms which may explain the law obtained. And finally we will transfer and apply these results in terms of NMR shifts to the oxidized state of HiPIP proteins, showing that they seem to constitute a good basis permitting the quantitative interpretation of their NMR spectra.

(1) Analysis of the Isotropic Hyperfine Couplings. The essential feature of the isotropic couplings in Table I (called A^i_{iso} in the following) is that they can be separated in two groups depending on their sign. The protons 5, 6, 7, and 8 belonging to the thiolate ligands bound to the irons 3 and 4 of the mixed-valence pair have *positive* isotropic couplings, while the protons 1, 2, 3, and 4 belonging to the ligands on the side of the pair of ferric atoms 1 and 2 have *negative* isotropic couplings. We estimate that these results are a direct consequence of the fact that the spin densities are positive on the irons 3 and 4 and negative on the ferric atoms 1 and 2. Moreover, the average value of the positive isotropic couplings (+2.42 MHz) of the protons 5, 6, 7, and 8 is greater than the average value of the negative isotropic couplings (−1.66 MHz) of the protons 1, 2, 3, and 4. These results suggest that each proton isotropic coupling of a particular ligand is related to the spin density present on the iron atom of the paramagnetic cubane bound to it and, more precisely, is proportional to it. This is thus the hypothesis that we adopt in the following. This hypothesis is in fact classical for the paramagnetic inorganic complexes and metalloproteins,[55,56] and it is an extension of the original model developed by McConnell in free radicals. However, these isotropic couplings must also depend on geometrical parameters related to the orientations of the Fe–S–C–H bonds in the ligands, and we will now examine this problem.

(2) Determination of the Empirical Law Relating Isotropic Couplings and Conformations. Since we have taken the above hypothesis as constitutive of our model, we have consequently normalized each proton isotropic coupling A^i_{iso} by the corresponding spin populations contained in Table IV. We thus obtain normalized couplings A^{*i}_{iso}, reported in Table IV, which are

(52) (a) Norman, J. G., Jr.; Ryan, P. B.; Noodleman, L. *J. Am. Chem. Soc.* **1980**, *102*, 4279. (b) Noodleman, L.; Baerends, E. J. *J. Am. Chem. Soc.* **1984**, *106*, 2316.

(53) Aizman, A.; Case, D. A. *J. Am. Chem. Soc.* **1982**, *104*, 3269.

(54) (a) Phillips, W. B.; Poe, M.; McDonald, C. C.; Bartsch, R. G. *Proc. Natl. Acad. Sci. U.S.A.* **1970**, *67*, 682. (b) Nettesheim, D. G.; Meyer, T. E.; Feinberg, B. A.; Otvos, J. D. *J. Biol. Chem.* **1983**, *258*, 8235. (c) Krishnamoorthi, R.; Markley, J. R.; Cusanovich, M. A.; Prysiecki, C. T.; Meyer, T. E. *Biochemistry* **1986**, *25*, 60. (d) Krishnamoorthi, R.; Cusanovich, M. A.; Meyer, T. E.; Prysiecki, C. T. *Eur. J. Biochem.* **1989**, *181*, 81. (e) Sola, M.; Cowan, J. A.; Gray, H. B. *Biochemistry* **1989**, *28*, 5261. (f) Cowan, J. A.; Sola, M. *Biochemistry* **1990**, *29*, 5633.

(55) La Mar, G. N.; DeW. Horrocks, W., Jr.; Holm, R. H. *NMR of Paramagnetic Molecules*; Academic Press: New York, 1973.

(56) Bertini, I.; Luchinat, C. *NMR of Paramagnetic Molecules in Biological Systems*; Benjamin-Cummings: Menlo Park, 1986.

relative to a spin population of +1 on each iron atom, so that

$$A^i_{iso} = D_S(Fe_i)A^{*i}_{iso} \quad (15)$$

These normalized couplings are all positive, by contrast with the A^i_{iso}, and they must depend only on the geometrical parameters defining the different Fe–S–C–H bonds. We have made the hypothesis that, in the present case, the A^{*i}_{iso} values depend only on one dihedral angle because the ligands in the crystallographic structure of the compound that we study are disposed in rather symmetric positions with respect to the cubane.[28] In effect, the Fe–S–C bonds respectively associated to the Fe_1 and Fe_2 atoms are contained in the same plane and they are nearly exactly symmetrically disposed with respect to the Fe_1–Fe_2 bisector plane. Due to the existence of an axis of quasi-symmetry very close to a $\bar{4}$ axis, the situation is the same for the Fe–S–C bonds associated with the Fe_3 and Fe_4 atoms. This means that the dihedral angles between the Fe–Fe–S and Fe–S–C bonds are all the same for the four ligands. However, this quasi-symmetry is lost at longer distances from the cubane, i.e. when the protons of the CH_2 groups and the carbons and hydrogens of the phenyls are considered. This is why we have defined the orientations of the CH_i bonds by the dihedral angles θ_i existing between the corresponding Fe–S–C and S–C–H_i planes in the Newman projections perpendicular to the S–C bonds. These θ_i, calculated from the X-ray structure,[28] have the following values: $\theta_1 = -43°$ for H_1, $\theta_2 = +80°$ for H_2, $\theta_3 = +11°$ for H_3, $\theta_4 = +126°$ for H_4, $\theta_5 = -1°$ for H_5, $\theta_6 = +120°$ for H_6, $\theta_7 = +22°$ for H_7, and $\theta_8 = +146°$ for H_8. They represent the only geometrical parameter contained in our problem, and we have searched for an empirical relation relating them to the normalized A^{*i}_{iso} values.[57] We have chosen an expression of the general form:

$$A^{*i}_{iso} = A + B\cos(\theta_i+\theta_0) + C\cos^2(\theta_i+\theta_0) \quad (16)$$

In this expression, these θ_i values are purely empirical parameters for the moment, with no particular meaning concerning the effective underlying mechanisms, and θ_0 is a supplementary reference angle meaning that we have made no preferential choice for the origin of the θ_i values. The expression 16 is not far from the $A + C\cos^2\theta$ expression often suggested,[16,54–56,58] but it contains in addition a term linear in cos θ similar to the one existing in the Karplus relation for the J_{AB} couplings in NMR. Its justification is that the local symmetry is low in the present problem, no symmetry plane existing perpendicular to the Fe–S bonds. By contrast, this linear term disappears by symmetry in the case of a C–H fragment of an aromatic radical.

With the help of a least square minimization procedure bearing on the four variables, A, B, C, and θ_0, and with the normalized isotropic couplings A^{*i}_{iso} of the protons 1, 3, 4, 5, 6, 7, and 8[59] given in Table IV and the corresponding θ_i, we have obtained the following expression (in Mhz):

$$A^{*i}_{iso} = 3.03 + 0.52\cos(\theta_i+\theta_0) - 2.28\cos^2(\theta_i+\theta_0) \quad (17)$$

with $\theta_0 = -21°$.

The corresponding curve is shown in Figure 4. The rather good fit between this law and the different experimental values indicates that the degree of transmission of the unpaired spin

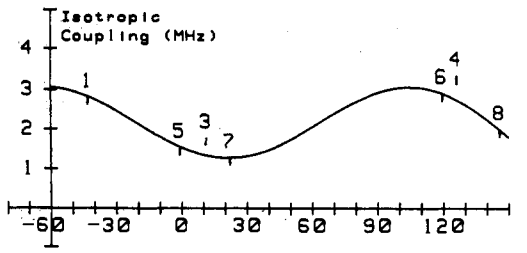

Figure 4. Representation of the empirical law relating the normalized experimental isotropic couplings A^{*i}_{iso} of the different protons to the dihedral angles θ_i defining the positions of these protons in the crystal. The law represented here corresponds to the expression 17.

density to the CH_2 protons seems independent from the nature of the iron atom attached to this ligand. This hypothesis seems to us quite reasonable for irons belonging to the same pair, i.e. the mixed-valence pair or the ferric plane. However, it is not evident that this law must be the same for the transmission of the spin density coming from irons belonging to two different pairs.[60] But, this seems approximately true here because, if the same fitting procedure is made with only the A^{*i}_{iso} values of the protons 5, 6, 7, and 8 related to the mixed-valence pair, we obtain

$$A^{*i}_{iso} = 2.95 + 0.48\cos(\theta_i+\theta_0) - 2.25\cos^2(\theta_i+\theta_0) \quad (18)$$

with $\theta_0 = -20°$, which is a very similar law to the previous one. Note also that the introduction of a θ_0 value different from zero seems useful, since, without it, the error function in these two minimization procedures is multiplied by 2.5.

Let us add a comment concerning the curious fact noted above that, in each CH_2 group, the proton which is the closest to the corresponding iron has the weakest magnitude of its isotropic coupling. This result comes from the interplay of the opposite signs associated with the major terms A and C of the expressions 17 and 18. In the particular case where the two protons of a CH_2 group are at the same distance from their corresponding iron atom, they are both defined by $|\theta_i| = 60°$, and they will have equal values $A^{*i}_{iso} = A + C/4$. If now these two protons are not at the same distance from the iron, due to the negative sign of C in (17) and (18), the closest one will correspond to the smallest $|\theta|$ value and thus to the smallest value of A^{*i}_{iso} and also the smallest value of $|A^i_{iso}|$.

(3) Analysis and Attempt to Interpret the Empirical Law Obtained. Three significant features emerge from the expressions 17 and 18: (i) The linear B term is the weakest. This term is nonzero for the reason mentioned above, but it is the smallest of the three parameters A, B, and C, as could be expected. (ii) The constant term A is greater than the C term. (iii) The sign of the C term is negative. The first observation is not astonishing, but the two others may appear surprising because they seem to be in contradiction with the classical expression $A + C\cos^2\theta_i$ where $A \ll C$ and C is positive. In effect, this positive sign of the C term is generally associated with an orbital overlap mechanism giving rise to an isotropic coupling which is maximum and positive for $\theta_i = 0$. But we want to point out that this apparent contradiction is the result of the choice that we have made above in taking the Fe–S bond directions as the origin of the θ_i angles. Other possible choices of the origin of θ can be made. They are related to different possible underlying mechanisms of transmission of the unpaired spin population toward the protons. We will discuss now these different possibilities.

The existing literature[55,56] considers that, in principle, two separate mechanisms of spin polarization and of delocalization by orbital overlap can be involved in order to explain the isotropic hyperfine couplings (or the paramagnetic NMR shifts) measured with the ligand nuclei. Moreover, concerning the delocalization mechanism which, by far, is the most often considered and

(57) The research of an empirical law relating the A^{*i}_{iso} and the θ values taken from the crystallographic structure relies on the supposition that the $[Fe_4S_4]^{3+}$ species studied here has atomic positions (and hence ligand conformations) very close to those corresponding to the original $[Fe_4S_4]^{2+}$ species present in the crystal and given in the X-ray study. This hypothesis is well legitimated by the results presented in Table IV, which show that, within the point-dipole approximation, we are able to reproduce fairly well the experimental tensors by calculations using the positions of the protons and the irons deduced from this crystallographic structure.

(58) Busse, S. C.; La Mar, G. N.; Howard, J. B. *J. Biol. Chem.* **1991**, *266*, 23714.

(59) Of course, the hyperfine tensor relative to proton 2 has not been used in order to determine the expression 17. In fact, the expression 17 obtained with the seven other protons was used to have an idea of the possible value of the isotropic coupling corresponding to proton 2.

(60) Noodleman, L. Private communication.

discussed, it distinguishes the possibilities of σ or π delocalization. Since these theoretical models constitute the framework of the analyses of all the measurements of this nature, we have to examine quantitatively these hypotheses in the present case in order to try to distinguish, if possible, the mechanism which is the most probable. However, it is important to be aware of the serious limits of these models, and even of their problematic adequacy when they are applied to a problem like the present one, i.e. of SCH_2 groups bound to high-spin iron atoms. In effect, in planar systems where σ and π orbitals are well defined and strictly separable by symmetry, the distinction between the σ and π delocalization mechanisms is clear-cut depending on the σ or π nature of the orbitals involved. Their difference is also very clear in experiments. The signature of the σ delocalization mechanism resides in the fact that the hyperfine couplings all show the same signs and decrease monotonically with the number of bonds separating the metal and the resonating nuclei while there is no decrease and there is sign alternation in the case of π delocalization. But apart from these simple situations, the things are much more approximate and not so clear. This is typically the case in the Fe–S–CH_i fragments that we consider here which, generally, are not planar and where several 3d iron orbitals containing unpaired electrons probably contribute to the delocalization process. Moreover, one must notice that hypotheses concerning the sulfur hybridization must be made if we want to compare the likelihood of these two possibilities, and these are the questions that we will examine in the following.

In the hypothesis of a π delocalization mechanism, each thiolate sulfur is considered as hybridized in sp^2, with its $3p_z$ orbital perpendicular to the Fe–S–C plane. Then, one must consider that a fraction of the spin population coming from the 3d orbitals of its vicinal iron is transferred by overlap to this $3p_z$ orbital which, in turn, will transfer by overlap a fraction of it to the 1s orbital of each hydrogen of the CH_2 groups. In this case, we have to define new dihedral angles, now called θ'_i, with respect to the new reference origin which is the axis of the $3p_z$ orbital, each θ'_i being equal to $\theta_i - \pi/2$. Then, in accordance with the supposed π symmetry, the θ_0 previously defined is neglected and the expression 17 approximately becomes

$$A^{*i}_{iso} = 0.75 - 0.52 \sin \theta'_i + 2.28 \cos^2 \theta'_i \qquad (19)$$

Since we find that the coefficient of $\cos^2 \theta'_i$ is now positive and also that the constant term is weaker than the last one, it appears that the hypothesis of a π delocalization mechanism is quite tenable. But it is not fully satisfactory, since the local symmetry does not correspond to π symmetry and since the hypothesis of π transmission between the Fe and S atoms remains problematic. Moreover, we must remark that the angles between the Fe–S and S–C bonds in these ligands are $104 \pm 2°$ in the crystallographic structure,[28] i.e. rather close to the sp^3 hybridization but far from the sp^2 hybridization.

This is why we have also considered the hypothesis of a σ delocalization mechanism. Then, the thiolate S atoms must be hybridized in sp^3, where, in fact, *three lone pairs have to be considered.* Let us point out that, in the previous paragraph, our definition of the origin of the θ_i corresponded implicitly to the choice that the unpaired spin population is contained, on these S atoms, in the particular lone pair pointing toward the direction of the iron atom ligated to it. This choice is traditional in the discussion of the σ delocalization mechanism concerning the ligand atom,[55] probably because, historically, the first examples treated dealt with transition metal complexes bound to nitrogen ligands which have only one lone electron pair. *But, by contrast with a recent analysis of this problem,[58] we think that, for sulfur ligands, the two other lone pairs (that we will call the two "external" lone pairs in the following) must be taken into consideration since they can also be the pertinent orbitals containing the unpaired spin density.*

Then, two questions arise: are these three lone pairs equivalent and what is the choice to make concerning the origin of the θ_i? The examination of our results in the framework of this hypothesis shows that *the two external lone pairs* (which are equivalent for reasons of symmetry) *must play a more important role in the determination of the values of the proton isotropic couplings than the one pointing toward the iron atom.* In effect, the values of these couplings are weaker for the protons 3, 5, and 7 than for the other protons and these three protons correspond to θ_i values close to zero (see also Figure 4). Since $\theta = 0$ corresponds to the maximum overlap with the lone pair pointing from the sulfur toward the iron atom, we must conclude that this lone pair seems to contain much less unpaired spin population than the two others. Consequently, the overlaps playing the essential role must be those occurring between the proton 1s orbitals and the two other external lone pairs of these sulfurs. This is why we have chosen—for reasons of symmetry—the internal bisector of the axes of these two external lone pairs as the new reference axis for the θ_i values. Since this axis has its projection in the Newman projection plane at 180° from the arbitrary reference axis previously chosen, we now obtain from (17) the following expression:

$$A^{*i}_{iso} = 3.03 - 0.52 \cos(\theta_i+\theta_0) - 2.28 \cos^2(\theta_i+\theta_0) \qquad (20)$$

with $\theta_0 = -21°$.

The term $\cos^2(\theta_i+\theta_0)$ continues to be negative in this expression, but this does not constitute a problem, since it does not correspond to the contribution of a single lone pair. But we have now to find what can be the form of the expression relative to each lone pair. To simplify this problem, we have now considered that $\theta_0 = 0$, that only the two external lone pairs play a role, and that they have their axis projections in the Newman projection plane at $\pm\beta$ with $\beta = 60°$ with respect to the reference axis. The contributions $A^{*i}_{iso}(+\beta)$ and $A^{*i}_{iso}(-\beta)$ to the isotropic couplings provided by each of these two lone-pair orbitals can then be written, forgetting here the subscript i:

$$A^{*}_{iso}(\pm\beta) = A_\beta + B_\beta \cos(\theta\pm\beta) + C_\beta \cos^2(\theta\pm\beta) \qquad (21)$$

Then

$$A^{*}_{iso} = A^{*}_{iso}(+\beta) + A^{*}_{iso}(-\beta)$$
$$= (2A_\beta + 2C_\beta \sin^2 \beta) + (2B_\beta \cos \beta) \cos \theta + (2C_\beta \cos 2\beta) \cos^2 \theta$$

Since $\beta = 60°$, we obtain

$$A^{*i}_{iso} = (2A_\beta + 3C_\beta/2) + B_\beta \cos \theta - C_\beta \cos^2 \theta \qquad (22)$$

The comparison of these expressions with the expression 20, gives us finally the approximate contribution corresponding to each external lone pair:

$$A^{*i}_{iso}(\pm\beta) = -0.20 - 0.52 \cos(\theta\pm\beta) + 2.28 \cos^2(\theta\pm\beta) \qquad (23)$$

In this expression the C_β term is now positive and much larger than the A_β term, as we expected. This corresponds to the fact that the unpaired spin population transferred must be minimum when $\theta \pm \beta = 90°$, i.e. when the overlap is minimum between the orbitals considered. The remark that A is greater than C in the expressions 17 and 18 is now explained. The reason is that the two external sulfur lone pairs both contribute to the transmission of the unpaired spin density toward a given proton. Then, the position of minimum overlap for one of them is not a position of minimum overlap for the other. Thus, it appears that the hypothesis of a σ delocalization mechanism is also quite tenable, provided that we suppose that the unpaired spin density is essentially contained in the two external lone pairs of the thiolate S atoms.

We conclude from these discussions that the two points of view corresponding to π or σ delocalization seem to us equally arguable and that we must appreciable their quite relative meaning. We have already emphasized that these two mechanistic models involve concepts that are necessarily only nonrigorous extensions of their original definitions. Let us also point out their approximate similarity, once taking into account that the two external lone pairs in the case of the σ delocalization mechanism are the important ones. In effect, in the Newman representation, the projections of the axes of the two external lone pairs corresponding to this σ delocalization hypothesis differ by only 30° from the axis of the two lobes of the $3p\pi$ orbital corresponding to the π case. Consequently, their overlaps with the 1s orbitals of the protons will be rather similar and the approximate similarity of the two hypotheses is not surprising. But it is also useful to recall at this stage that the concurrent mechanism of spin polarization, which may also play a role in the transmission of the spin population to the CH_2 protons, has been evoked only and not really taken into account due to the lack of a serious model for the orientational dependence of this last mechanism. Finally therefore, we propose that one should not favor too much one model (σ or π) with respect to the other; rather one should see them as two approximate and relatively equivalent views of this subject.

Then, we consider that the empirical formulas 17 and 18 remain more significant than their unavoidably ambiguous interpretations, and these are the formulas that we will retain now, when coming to the interpretation of the paramagnetic NMR shifts of the CH_2 groups in the proteins.

(4) Relation between These Isotropic Couplings and the ^1H Paramagnetic Shifts in the NMR Spectra of Oxidized HiPIP Proteins. High-potential (HiPIP) ferredoxin proteins, especially from *Chromatium*, have already been studied by proton NMR in solution and particularly in their oxidized state where their active site is in the $[Fe_4S_4]^{3+}$ state.[13-17,54] Their characteristic feature is to exhibit lines with large positive and negative shifts attributed to the β-CH_2 protons of their cysteine ligands, outside the 0–10 ppm range. Their large shifts are due to the paramagnetism of the Fe–S cluster, via the electron–nuclear hyperfine interaction between the electron spin distribution and the protons considered. Consequently, there must be a direct relation between these NMR shifts $\delta\nu_i/\nu$ and the isotropic hyperfine couplings A^i_{iso} that we have deduced from our ENDOR measurements. For the simple case of a single occupied pure spin $S = {}^1/_2$ orbitally nondegenerate state, the relation[61] would be

$$(\delta\nu_i/\nu)_{para} = g\beta_e/4g_H\beta_H kTA^i_{iso} \qquad (24)$$

Note that the A^i_{iso} values contain both the Fermi contact term and the so-called dipolar shift contributions. However, the contact term is, here, largely preponderant, as it can be estimated from the discussions in Section IV-2 showing, for the CH_2 protons, the smallness of the orbital contribution to their hyperfine interactions with respect to those, isotropic or anisotropic, associated with the electron spins.

Consequently, the empirical law that we have determined above from the ENDOR measurements represents a new possibility to give a quantitative interpretation of the β-CH_2 proton shifts in these proteins. However, we must be aware that the direct transcription of our ENDOR hyperfine couplings in terms of NMR shifts with the help of expression 24 corresponds to an approximation. In effect, our ENDOR measurements have been made around 10 K. Thus, they only determine the contribution to these shifts coming from the fundamental spin state. By contrast, the NMR experiments are made at room temperature. The approximation that we will make at the present stage consists of neglecting the eventual contributions to the NMR shifts coming from excited spin states possibly populated at room temperature. Under this assumption, if we imagine a hypothetical NMR experiment made in solution at $T = 300$ K corresponding to the unchanged proton CH_2 isotropic couplings of center IV, their NMR lines would be given by the expression

$$\delta\nu_i/\nu = (\delta\nu_i/\nu)_{dia} + (\delta\nu_i/\nu)_{para} = 3 + 26.3A^i_{iso}\ (\text{in ppm}) \qquad (25)$$

where the NMR shifts will have the same signs as the proton isotropic hyperfine couplings, due to the positive sign of the coefficient in the expression 24.

Using this expression and the isotropic couplings contained in Table I, we have thus calculated their corresponding (hypothetical) NMR shifts at 300 K. Four lines are predicted with large positive shifts. They correspond to the protons H_5–H_8 on the side of the mixed-valence pair. Their values calculated with the expression 25 are $\delta_5 = +52$ ppm, $\delta_6 = +99$ ppm, $\delta_7 = +45$ ppm, and $\delta_8 = +71$ ppm, and their average value is +66 ppm. By contrast, four lines are predicted with negative shifts and of smaller magnitude than the previous ones. They correspond to the protons H_1–H_4 on the side of the ferric pair, and their calculated values are $\delta_1 = -48$ ppm, $\delta_2 = -45$ ppm, $\delta_3 = -24$ ppm, $\delta_4 = -49$ ppm while their average value is –41 ppm.

Let us come now to the NMR spectra of the oxidized HiPIP proteins.[14-16,54] Important similarities appear between the positions of the eight lines that diverse authors have attributed to the β-CH_2 protons of cysteines and those calculated above from our model. Four of these lines are generally present in the same range of positive shifts as above, while between two and four lines, depending on the protein,[62] are found in a zone of negative shifts with, however, somewhat smaller values than above. Thus, at a global level, there is a rather good agreement between the values coming from our model system and those of the proteins. Of course, the particular values found for the different proteins and for our model cannot be compared in detail, since the angles defining the conformations of the CH_2 groups inside the ligands will generally differ in every case. However, the observation of this global agreement and its combination with the assignments that we have made for our model lead us, by transposition to the proteins, to an important conclusion. This conclusion is that, *in these proteins, the NMR lines which have the positive paramagnetic shifts in the NMR spectra must be identified with the protons of the CH_2 groups attached to the irons of the mixed-valence pair, while those which are attached to the two ferric irons do correspond to the lines having negative paramagnetic shifts* (with, however, the restriction evoked in ref 62).

The present assignment which is deduced from these studies of this synthetic model and is then applied to the proteins corroborates and certifies by an independent way the assignments that Bertini et al. have recently proposed for the oxidized state of the *Chromatium* protein.[13] These authors obtained their assignments for their part by a purely NMR approach based on the comparison of the "Curie" or "anti-Curie" slopes of the line positions as a function of temperature.

But the results of the present study lead us to put forward some additional proposals concerning the detailed analysis of the NMR spectra of the proteins. The first one is that we propose to consider the empirical formula 17 (or 18) as the basis for the quantitative interpretation of the angular dependence of the paramagnetic shifts of the NMR lines of the CH_2 groups in the oxidized state of these proteins. And our second proposal is that the spin state

(61) When the fundamental state and also excited spin states are populated at room temperature, the paramagnetic shifts will be the sum of several expressions like (24), multiplied by the distributions of their different populations.

(62) Here, the comparison between the NMR lines in the proteins and those predicted by the results of this paper can only be global and qualitative. This is why, at this stage of the discussion of the NMR spectra of the proteins, we have not taken into account the particular features present in *Rhodocyclus gelatinosus* and *C. vinosum* (see refs 17 and 18), and their recent discussion in ref 15, where, by comparison with *Ectothiorhodospira halophila*, two NMR lines appear to have shifted from the negative to the positive ppm side.

of the $[Fe_4S_4]^{3+}$ active sites of the oxidized high-potential proteins—under the experimental conditions relevant to their NMR studies—appears to be $|^7/_2,3,^1/_2\rangle$ and not $|^9/_2,4,^1/_2\rangle$ as it has been previously supposed.[14] This last conjecture relies primarily on the good agreement between our postulated NMR shifts and those found in the proteins. But the results that we have obtained very recently on center I also confirm it[5] (see the Note Added in Proof, at the end of the Conclusion of the present article).

However, it is important to recall the limits of these conclusions. The first one is that we have treated a particular case where the isotropic hyperfine couplings of the CH_2 protons depend only on two parameters, $D_S(Fe_i)$ and θ_i. More generally, it might be necessary to introduce a second angular parameter, since these couplings may also depend on the orientations of the S–C bonds with respect to those of the relevant 3d orbitals on the iron atoms. A second limitation in our attempt to interpret the NMR spectra of the proteins at 300 K is that we have only considered the fundamental spin state on which we have obtained precise information by ENDOR around 10 K. The fact that a satisfactory agreement is already obtained when only the fundamental state is considered may signify that the excited spin states are not very close to this fundamental state in the oxidized high-potential proteins studied. An indirect indication supporting this hypothesis is that the **g** tensor of center IV does not changing appreciably between 4 and 30 K. Thus, at least for this center IV, excited states are not very close to the fundamental one. However the possibility remains in the model as well as in the proteins that excited states may play a role at higher temperatures and typically at room temperature. The agreement discussed above would subsist if they were only weakly populated at this temperature. But we want to suggest another possibility able to explain in a satisfying way the agreement observed. This possibility is that the two excited states $|^9/_2,4,^1/_2\rangle$ and $|^5/_2,2,^1/_2\rangle$ might be appreciably populated at room temperature, but with their contributions compensating each other. In effect, concerning the $|^9/_2,4,^1/_2\rangle$ state, the CH_2 protons on the side of the mixed-valence pair must give rise to positive paramagnetic shifts *greater* than those in the case of the $|^7/_2,3,^1/_2\rangle$ state, while those on the side of the ferric pair must also give rise to *greater* negative shifts. On the contrary, if we now consider the $|^5/_2,2,^1/_2\rangle$ state, the first category of protons will give positive paramagnetic shifts *smaller* than those with the $|^7/_2,3,^1/_2\rangle$ state, and the second one *smaller* negative shifts. Consequently, it is possible to imagine that the energy levels corresponding to these two excited magnetic states may be disposed in such a way on an energy scale that their effects approximately compensate to give rise to NMR lines roughly centered on the values corresponding to the fundamental $|^7/_2,3,^1/_2\rangle$ state.

Thus, it must be clear that the present propositions only represent a first attempt, relative to the oxidized state of the high-potential proteins, toward obtaining quantitative models able to interpret the β-CH_2 NMR shifts in the iron–sulfur proteins. Future progress on this problem is expected from similar studies that we undertake on other paramagnetic centers in these irradiated crystals.

(VI) Conclusions

The work described in this article corresponds to the measurement by ENDOR of the hyperfine tensors of the protons of the CH_2 groups in a paramagnetic $[Fe_4S_4]^{3+}$ species called "center IV", created by γ irradiation in single crystals of the synthetic model compound $[N(C_2D_5)]_2[Fe_4S_4(SCH_2C_6D_5)_4]$. The study of this paramagnetic center is biologically relevant, and this will be discussed in more detail in a forthcoming publication.[4] In effect, the comparison of the **g** tensor of center IV with those of certain high-potential proteins in their oxidized state shows their similarity.[63,64]

With the help of the analysis—by the point-dipole approximation—of the anisotropic part of the proton hyperfine tensors being measured, it has been possible to obtain the distribution of the electron spin populations $D_S(i)$ on the iron and sulfur atoms of the cluster. These new results lead us to the identification of the species studied as being in the magnetic spin state $|^7/_2,3,^1/_2\rangle$. This identification is given within the framework of the model used in the literature for the discussion of the previous Mössbauer results, i.e. the pure valence-bond approximation with the spin populations entirely relocalized on the magnetic iron atoms. This attribution contrasts with the previous one which considered that the fundamental spin state of $[Fe_4S_4]^{3+}$ is $|^9/_2,4,^1/_2\rangle$.[38] The assignment of the fundamental spin state $|^7/_2,3,^1/_2\rangle$ is also important because we estimate that it must be extended to the interpretation of the Mössbauer and NMR spectra of the oxidized high-potential proteins.

The last category of significant new results presented in this article deals with the analysis of the isotropic part of the hyperfine tensors of the eight protons. Finally, they can be summarized into the following formula:

$$A^j_{iso}\ (\text{in MHz}) = D_S(Fe_i)\{3 + 0.5\cos(\theta_j - 20°) - 2.3\cos^2(\theta_j - 20°)\} \quad (26)$$

where A^j_{iso} is the isotropic coupling of proton j, $D_S(Fe_i)$ is the electron spin population on its adjacent iron i, and θ_j defines the orientation of the C_i–H_j bond with respect to the corresponding S_i–C_i one. This law corresponds to the combination and simplification of our previous expressions 15, 17, and 18. It has been deduced from the isotropic couplings of the two groups of four protons: those on the side of the mixed-valence pair and also those on the side of the ferric pair. This does not imply in our mind that the law is, in general, surely the same for these two categories of protons; we will have to examine more closely this problem in the future. However, we feel that the expression 26 obtained here for center IV can constitute a first basis and, we hope, a good one for the quantitative interpretation of the paramagnetic shifts in the NMR spectra of high-potential proteins in their oxidized state. But, here again, other studies on similar systems will be necessary in order to assess its exact relevance.

Finally, we hope that this ENDOR study will be not only fruitful per se, in consideration of the new knowledge obtained, but also a little beyond. First, it may contribute to a more unified view with respect to the determination of the spin populations between the domains of free radicals, of transition metal ions, and of their polymetallic complexes. Second, more specifically about iron–sulfur cubanes, we hope to have established fruitful connections between these results and those issued from Mössbauer and NMR, giving us the possibility to propose new, unified and quantitative interpretations on the $[Fe_4S_4]^{3+}$ state in the model compounds as well as in the proteins.

Note Added in Proof. As it has been said in the Introduction, nearly completed studies of a second paramagnetic $[Fe_4S_4]^{3+}$ center (called center I) have been performed in the same crystals.[5] We just want to mention rapidly here some salient results on it

(63) Let us briefly comment on this point here. The most interesting case is related to the complex EPR spectrum observed in oxidized *C. vinosum* which has been interpreted as the superposition of two main components (see ref 7a). The first one corresponds to an axial **g** tensor ($g_1 = 2.12$, $g_2 = g_3 = 2.04$) with easily saturable lines, while the second one corresponds to a rhombic and less anisotropic **g** tensor ($g_1 = 2.088$, $g_2 = 2.055$, and $g_3 = 2.040$) which is much less saturable. We notice that the center IV studied here has properties rather close to those of the second, rhombic set of EPR lines. By contrast, we will see that center I and also center II, which are other $[Fe_4S_4]^{3+}$ centers present in our irradiated crystals have EPR properties fairly similar to those of the first set of EPR lines in the protein. Let us also add that the anisotropy of the **g** tensor of center IV and its average g value are also fairly comparable to those of the oxidized *E. halophila* high-potential protein (see ref 64).

(64) Beinert, H.; Thomson, A. J. *Arch. Biochem. Biophys.* **1983**, *222*, 333.

which, when compared to those on center IV, *do confirm the analyses presented here on the center IV, especially concerning the assignment that the $|^7/_2,3,^1/_2\rangle$ spin state is its fundamental state.* The proton tensors obtained for center I demonstrate that its mixed-valence pair is localized on the iron atoms 2 and 3. But their magnitudes are greater in mean value than those obtained for center IV. This leads to spin populations which are roughly 15% greater in center I than in center IV for the mixed-valence pair of irons, while they are 60% greater in center I than in center IV for those on the ferric pair. Following the discussion of Section IV-6, we come to the conclusion that the fundamental magnetic state of this center I must be identified with the $|^9/_2,4,^1/_2\rangle$ state. Consequently, the comparison of the results belonging respectively to the centers I and IV does confirm that the center IV studied in this article must be identified with the $|^7/_2,3,^1/_2\rangle$ spin state.

Moreover, preliminary but still incomplete ^{57}Fe ENDOR measurements made on center I allow us to deduce the following order of magnitude for the ^{57}Fe isotropic hyperfine interactions: $A(Fe^{2.5+}) = -37 \pm 3$ Mhz for the iron of the mixed-valence pair and $A(Fe^{3+}) = +28 \pm 2$ Mhz for the irons of the ferric pair. These numbers are in very good agreement with the values of respectively −38.5 and +26.7 Mhz predicted for the $|^9/_2,4,^1/_2\rangle$ state (see Section IV-5). Thus, they represent a supplementary confirmation that the fundamental spin state of center I is the $|^9/_2,4,^1/_2\rangle$ state while the $|^7/_2,3,^1/_2\rangle$ state corresponds to the fundamental spin state of center IV.

Last, it is possible to calculate, in the same way as in Section V-4, what would be the positions of the (hypothetical) NMR lines relative to the center I with the help of the expression 25 and with the spin populations on its different irons just evoked above. They correspond to large positive shifts (between +100 and +40 ppm, with an average value of +68 ppm) for the NMR lines of the CH_2 protons on the side of the mixed-valence pair and to *large negative shifts* (between −90 and −50 ppm, with an average value of −69 ppm) for the NMR lines of the CH_2 protons on the side of the ferric pair. The origin of these last large negative shifts is due to the fact that the negative unpaired spin populations appearing on the two irons of the ferric pair are much larger in the $|^9/_2,4,^1/_2\rangle$ state case than in the $|^7/_2,3,^1/_2\rangle$ case. Since such large negative shifts do not appear in the NMR spectra of the different oxidized high-potential proteins already studied, we estimate that this constitutes a supplementary argument in favor of the proposition that the $|^7/_2,3,^1/_2\rangle$ state is the fundamental state of the active sites of these proteins, with respect to their NMR studies.

Acknowledgment. We want to thank Dr. Louis Noodleman and Prof. David Case from the Research Institute of Scripps Clinic (La Jolla, CA), Prof. Patrick Bertrand (University of Provence, Marseille, France), Prof. Robert Subra (University Joseph Fourier, Grenoble), Prof. Claudio Luchinat (University of Bologna, Italy), and our colleagues Dr. Jacques Gaillard and Dr. Pascal-Henry Fries for numerous and very interesting discussions on various parts of this work. We are also indebted to Mr. Gerard Desfonds and Mr. Gerard L'Hospice for their help in the material realization of this work and to Dr. Jean-Pierre Noël from the Service des Molécules marquées in Saclay (CEA) and our colleague Dr. Hervé Bazin for their good advice concerning the syntheses and the isotopic labeling. And finally we want to thank NATO for a Collaborative Research Grant (CRG 910204), which allowed us to establish an organized collaboration with Dr. Louis Noodleman and Prof. David Case on these problems.